Upstream open reading frames dynamically modulate CLOCK protein translation to regulate circadian rhythm and sleep

Yuanqiang Sun[1,#], Ke Shui[2,3,#], Qinyu Li[3], Chenlu Liu[1], Wanting Jin[1], Jian-Quan Ni[4], Jian Lu[1,*], Luoying Zhang[3,5,*]

[1] China State Key Laboratory of Protein and Plant Gene Research, Center for Bioinformatics, School of Life Sciences, Peking University, Beijing 100871, China

[2] College of Biomedicine and Health, College of Life Science and Technology, Huazhong Agricultural University, Wuhan, Hubei 430070, China

[3] Key Laboratory of Molecular Biophysics of Ministry of Education, College of Life Science and Technology, Huazhong University of Science and Technology, Wuhan, Hubei, 430074, China

[4] Gene Regulatory Lab, School of Medicine, Tsinghua University, Beijing, China.

[5] Hubei Province Key Laboratory of Oral and Maxillofacial Development and Regeneration, Wuhan, Hubei 430022, China

#These authors contributed equally to this work.

*Corresponding author.

Email: luj@pku.edu.cn (Jian Lu); zhangluoying@hust.edu.cn (Luoying Zhang)

Author Contributions: J.L. and L.Z. initiated the project and oversaw all aspects of the project. With the help of Q.L. and J.N., Y.S., K.S., C.L. and W.J. performed research and analyzed data; J.L. and L.Z. wrote the manuscript with input from all the authors.

Competing Interest Statement: The authors declare no competing interests.

Classification: Biological Sciences, Neuroscience

Keywords: circadian rhythm, *Clock*, uORF, sleep, *Drosophila*,

Abstract

The circadian rhythm is an evolutionarily conserved mechanism with translational regulation increasingly recognized as pivotal in its modulation. In this study, we found that upstream open reading frames (uORFs) are enriched in circadian rhythm genes, with particularly conserved uORFs present in core circadian clock genes. We demonstrate evidence that the uORFs of the core clock gene, *Clock* (*Clk*), rhythmically and substantially attenuate CLK protein translation in *Drosophila*, with pronounced suppression occurring during daylight hours. Eliminating *Clk* uORFs results in elevated CLK protein levels during the day and a compressed circadian cycle, along with a broad shift in clock gene expression rhythms. Interestingly, *Clk* uORF deletion also augments morning sleep by reducing dopaminergic activity. Beyond daily circadian adjustments, *Clk* uORFs play a role in modulating sleep patterns in response to the varying day lengths of different seasons, inhibiting translation in a day-length contingent manner. Furthermore, the *Clk* uORFs act as a master regulator to shape the rhythmic expression of a vast array of genes and influence multifaceted physiological outcomes. Collectively, our research sheds light on the intricate ways uORFs dynamically adjust downstream coding sequences to acclimate to environmental shifts.

Introduction

Circadian rhythms orchestrate ~24-hour cycles in a multitude of biological processes, with the sleep-wake cycle being a particularly salient manifestation. The molecular underpinnings of the circadian rhythms consist of a transcription-translation feedback loop (TTFL), an evolutionarily conserved mechanism evident across diverse taxa, ranging from bacteria to fungi, plants, and animals [1-4]. The circadian systems drive gene expression rhythms of thousands of genes, exerting pervasive influences on daily fundamental biological activities from the cellular level to complex behaviors and diseases such as cell proliferation, cell signaling, metabolism, rest/activity, cancer and neurodegeneration [5-7]. Despite shared rhythmic principles in the tree of life, species-specific divergence in clock components and mechanisms is evident, likely a result of distinct environmental pressures and life histories shaping unique adaptations after a single origin in a common ancestor of all life forms [4,8]. Alternatively, the difference in genetic components across different kingdoms of life implies that these rhythmic systems probably emerged separately in various lineages at an early stage via convergent evolution [9,10]. While the key genetic components that drive the circadian rhythms have been deciphered [5-7], the intricate regulatory mechanisms fine-tuning these rhythms remain partially obscured, with significant gaps in our understanding persisting.

Drosophila, with its genetic tractability and conservation of key circadian components, serves as an unparalleled model providing profound insights that resonate across species, including humans [4,11-14]. In *Drosophila*, two transcriptional activators, CLOCK (CLK) and CYCLE (CYC), constitute the positive limb of the loops. CLK and CYC heterodimerize and activate the transcription of *period* (*per*) and *timeless* (*tim*) via E-box enhancer elements [15,16]. As PER and TIM proteins accumulate in the cytoplasm, they bind to each other and translocate into the nucleus to suppress the transcriptional activities of CLK and CYC, thus repressing their own transcription and forming a pivotal negative feedback loop [17]. Throughout this process, the stoichiometry of these core regulators is precisely controlled to ensure the accuracy of the circadian rhythms. For instance, the overexpression of CLK-CYC increases their activity at *per* and *tim* E-box enhancers, consequently shortening the circadian rhythms [18,19]. Recent studies have revealed that the precision of circadian rhythms is regulated by multi-layered mechanisms beyond transcriptional modulation, which include the regulation of protein synthesis and post-translational stability. For instance, the translation of *tim* and *per* mRNAs is facilitated by TWENTY-FOUR and its activator, ATAXIN2, through their promotion of an association with polyadenylate-binding protein [20-23]. Additionally, the synthesis of CLK and TIM proteins is inhibited by the microRNAs *bantam* [24] and *mir-276a* [25], respectively, with the overexpression of either miRNA leading to prolonged periods or arrhythmicity [24-26]. Post-translational modifications (PTMs) also affect the stability and subsequent degradation of PER and TIM [1].

While recent advances have significantly enhanced our understanding of the regulatory complexity of the classical TTFL, the field has not yet completely elucidated the intricate network of components and interactions that govern the fine-scale regulation of circadian rhythms, even in *Drosophila*, the quintessential model for circadian biology.

Recent studies underscore the pivotal role of translational regulation, particularly by upstream open reading frames (uORFs), in the control of circadian rhythms in organisms with divergent circadian architectures. uORFs, the short ORFs with start codons located within the 5' untranslated regions (5'UTRs) of eukaryotic mRNAs, are widely distributed in eukaryotic genomes [27]. uORFs play a key role in suppressing translation initiation of the downstream coding sequence (CDS) in an mRNA by either sequestering ribosomes or competing for binding to translation initiation complexes [28-32]. In *Neurospora*, the central circadian clock component, *frequency* (*frq*), has two isoforms—large (l-FRQ) and small (s-FRQ)—whose balance is determined by temperature-dependent splicing and is essential for the temperature compensation of circadian rhythms. Thermosensitive trapping of scanning ribosomes at the uORFs of l-FRQ modulates FRQ protein levels in response to ambient temperatures, thus calibrating the circadian clock [33]. Similarly, TIMING OF CAB EXPRESSION 1 (TOC1), a core component of the *Arabidopsis* circadian clock, is regulated by uORFs within its mRNA leader sequence [34]. Although *Neurospora* and *Arabidopsis* share similar design principles in circadian rhythms as humans and flies, the proteins involved differ significantly in both structure and conservation [35-37]. Recent studies have shown that uORFs in the mouse core clock gene *Period2* (*Per2*) play a role in temperature entrainment of the circadian clock [38] and in regulating sleep [39]. However, no significant differences in the period and amplitude of circadian rhythms were observed between wild-type and *Per2* uORF mutant mice [39]. In addition, extensive ribosomal binding to uORFs in rhythmically expressed mRNAs has been observed in mammalian cells, yet the functional impacts of these uORFs in circadian regulation have not been characterized [40,41]. In summary, although research into the translational regulation by uORFs is burgeoning, the complete spectrum of regulatory functions of uORFs in circadian rhythm control remains to be elucidated. Moreover, the potential impacts of uORF-mediated regulation on physiological and pathological processes linked to circadian rhythms are currently elusive, while their delineations can help reveal how circadian rhythms adapt to environmental pressures.

Here, we show that circadian rhythm-related genes are significantly enriched with ultra-conserved uORFs in *Drosophila*. These uORFs, which demonstrate translational activity in our previously published translatome data [42], thus may play a crucial role in modulating circadian rhythms. We then conducted an in-depth exploration of conserved and potentially functional

uORFs in *Clk* of *Drosophila melanogaster* and presented evidence that these uORFs substantially inhibit protein translation *in vitro* and *in vivo*. Knocking out (KO) *Clk* uORFs amplifies daytime CLK protein levels and shortens the circadian period of locomotor rhythm. Furthermore, *Clk*-uORF-KO mutants manifest increased morning sleep, likely stemming from diminished dopaminergic activity. These mutants also exhibit defects in modulating sleep duration in response to photoperiodic shifts. Molecular investigations underscore the requirement of *Clk* uORFs for photoperiod-driven regulation of CLK protein, highlighting their central role in both circadian and circannual orchestrations. Intriguingly, the mutants also display decreased fecundity and diminished resilience to starvation, indicating that the ablation of *Clk* uORFs has extensive physiological consequences beyond the regulation of circadian rhythms and sleep.

Results

Circadian rhythm genes are more likely to be regulated by uORFs

We identified 36,565 putative canonical uORFs across all isoforms of 13,470 protein-coding genes in *D. melanogaster*. Of these, 1,137 uORFs are associated with 169 circadian rhythm-related genes (GO:0007623), demonstrating a significant enrichment of uORFs in this category of genes ($P < 10^{-16}$, Fisher's exact test; Fig. 1A). Since conserved uORFs are more likely to be functional, we then focused on uORFs highly conserved across *Drosophila* species. As the start codon (uATG) is the most pivotal and definitive feature of a canonical uORF [30,43], we investigated the conservation patterns of the uATGs based on the multiple sequence alignments (MSA) of 23 *Drosophila* species. This analysis revealed 388 uATGs (within 250 genes) that are identical across the *Drosophila* species examined (Table S1). These genes are significantly enriched for functions in neuronal axon genesis and transcriptional regulation, implicating the potential roles of uORFs in modulating these processes (Fig. S1). Among the 169 circadian rhythm-related genes, 29 uORFs display conservation of uATGs, a higher ratio than that of uORFs in the remaining genes (29/1,137 vs. 359/35,428; $P = 2.3\times10^{-5}$, Fisher's exact test; Fig. 1B). For the ten core clock genes (Table1), we found that 7 out of 82 uORFs possess uATGs that are identical across *Drosophila* species, suggesting higher uORF conservation in the core versus other circadian genes (7/82 vs. 22/1,055; $P = 0.005$, Fisher's exact test; Fig. 1B). These seven conserved uORFs are distributed among four genes, with *Pdp1* containing four, and *Clk*, *sgg*, and *cwo* each containing one (Table 1). These patterns suggest that circadian rhythm genes, especially core clock genes, are more inclined to be regulated by uORFs.

Besides conservation, the regulatory functions of uORFs are also implied by their expression and translation patterns. Analysis of our previously published transcriptome and translatome data [42] indicates that 78% of the 1,137 uORFs in the circadian rhythm-related genes

are expressed in adult heads (mRNA RPKM > 0.1, 888 in males and 879 in females; Table 1), and about 80% of these expressed uORFs display evidence of translation [Translation efficiency (TE) > 0.1, 692/888 in males and 714/879 in females; Table 1]. Notably, 25 of the 29 highly conserved uORFs exhibit translation signals in the heads of both sexes. Of the 82 uORFs from the core clock genes, 60% show mRNA expression in adult heads (67 in males and 63 in females), with 78% of these expressed uORFs exhibiting translation signals (52/67 in males and 49/63 in females; Table 1), suggesting their potential functional importance.

To assess the impact of uORFs on translation efficiency of the downstream CDS, we categorized the circadian rhythm-related genes expressed in heads (149 in male and 147 in female) into three groups: Class I (genes with conserved uORFs that are translated, 12 in male and 12 in female), Class II (genes with translated uORFs that are not highly conserved, 98 in male and 100 in female), and Class III (genes without translated uORFs, 39 in male and 35 in female). We observed that genes with translated uORFs (Class I and II) overall display a lower TE than those without (Class III) ($P < 0.0002$ for both male and female heads, respectively, Wilcoxon signed-rank test; Fig. 1C). While not statistically significant, Class I genes show a tendency of lower TE compared to that of Class II in both sexes. Each of the four core clock genes (*Clk*, *cyc*, *per*, and *tim*) demonstrated reduced TE relative to the genomic average. Notably, *Clk* belongs to Class I and exhibits a significantly lower TE, implying a substantial regulatory impact of uORFs on its translation (Fig. 1C).

uORFs suppress CLK and CYC translation *in vitro* and *in vivo*

In *Drosophila melanogaster*, the 5'UTR of *Clk* mRNA contains five canonical uORFs, among which the second (uORF2) and the third uORF (uORF3) are in-frame to each other and overlapping (Fig. 2A). Among the five uORFs of *Clk*, the start codon of uORF2 (uATG2) is the most conserved, identical across all 23 *Drosophila* species (Fig. 2A). As CYC is the binding partner of CLK, we also analyzed *cyc* for comparison. The 5'UTR of *cyc* mRNA contains four canonical uORFs (SI Appendix, Fig. S2A). The uATGs of *cyc* are less conserved than those of *Clk* in general, and none of them is identical across the 23 *Drosophila* species (SI Appendix, Fig. S2A). We detected prominent mRNA expression and ribosome occupancy for uORF2 and uORF3 of *Clk* in the head and body of male and female flies (Fig. 2B). As for *cyc*, prominent mRNA expression and ribosome occupancy was observed for uORF2, uORF3 and uORF4 (SI Appendix, Fig. S2B).

To further explore the regulatory impact of these uORFs on CDS translation, we performed a dual-luciferase reporter assay *in vitro*. We engineered dual-luciferase constructs with either wild-type (WT) or mutated 5'UTRs of *Clk* and *cyc* mRNAs, where the start codons for *Clk*

197 uORF2 and uORF3, as well as *cyc* uORF2, uORF3, and uORF4, were mutated from ATGs to
198 ATTs (Fig. 2C). In *Drosophila* S2 cells, we observed that the luminescence intensity, indicative
199 of CDS translational activity, was more than 70% higher in constructs with mutated 5'UTRs
200 compared to WT controls (WT vs. mutant: 1 vs. 1.79 and 1 vs. 1.83 for *Clk* and *cyc* 5'UTR,
201 respectively; $P < 0.001$ for 5'UTRs of both *Clk* and *cyc*; Fig. 2C). This significant increase
202 confirms the repressive function of these uORFs on the translation of downstream CDSs.
203
204 To investigate the function of *Clk* and *cyc* uORFs *in vivo*, we knocked out *Clk* uORF2 and
205 uORF3 simultaneously by mutating their start codon ATGs to ATTs, and established a
206 homozygous knock-out line (*Clk*-uORF-KO) (Fig. 2D). Similarly, we mutated the ATG start
207 codons of uORF2-4 to ATTs in *cyc* and generated a homozygous knock-out line (*cyc*-uORF-
208 KO) (Fig. 2D). We carried out ribosome fractionation followed by quantitative PCR (qPCR) to
209 compare the mRNA abundance in the polysome fraction to that in the monosome fraction (P-
210 to-M ratio) for *Clk* and *cyc*, respectively (Fig. S3). A larger P-to-M ratio means more mRNAs
211 are enriched in the polysome fractions and bound by more ribosomes, thus indicative of higher
212 translation efficiency [44-46]. We conducted experiments on male heads from *Clk*-uORF-KO, *cyc*-
213 uORF-KO, and WT flies at various Zeitgeber times (ZT), starting from ZT0 (the onset of lights)
214 to ZT20 at 4-hour intervals. P-to-M ratios of *Clk* mRNA in *Clk*-uORF-KO flies significantly
215 exceeded WT at ZT0, ZT4, and ZT8, with no notable changes at ZT12 and ZT16, and a decrease
216 at ZT20 (Fig. 3A). Conversely, P-to-M ratios for *cyc* mRNA in *cyc*-uORF-KO flies were
217 slightly higher at all but one ZT time point (ZT12) (Fig. 3B). Notably, the elevation in *cyc*
218 mRNA was not statistically significant except at ZT16. Overall, these patterns indicate *Clk*
219 uORFs exert a substantial impact on translation, especially during the light phase, while *cyc*
220 uORFs show modest effects. Consequently, our research has pivoted to focus on *Clk* uORFs.
221
222 Next, we measured CLK protein abundances for male and female heads at different time
223 points using immunoblotting (Fig. 3C and 3D). We found that CLK protein levels were
224 significantly higher in the heads of male *Clk*-uORF-KO flies compared to WT during the
225 morning hours of ZT0, ZT4, and ZT8, and marginally lower, though not significantly, at ZT16
226 and ZT20 (Fig. 3E). Similar patterns were observed for female heads (Fig. 3F). These protein
227 abundance trends corroborate the enhanced translational activity in *Clk*-uORF-KO mutants
228 compared to WT during the light phase. Overall, the data demonstrate that *Clk* uORFs
229 downregulate CLK protein translation during the daytime, with pronounced effects observed in
230 the early hours.
231
232 ***Clk* uORFs modulate the pace of the circadian clock**
233 To quantitatively assess the effects of *Clk* uORF KO on circadian rhythms, we utilized a

234 mathematical model previously established for simulating the *Drosophila* molecular clock [47].
235 This model employs nonlinear ordinary differential equations to model the regulatory weights
236 among mRNA and protein molecules within the circadian network, making it applicable for
237 predicting the increase in *Clk* translation when uORFs are disrupted. By incrementing the
238 regulatory weight from *Clk* mRNA to CLK protein from the baseline to higher values, we
239 incorporated the anticipated enhancement in *Clk* translation due to the uORF KO into our model
240 (Fig. 4A).
241
242 The simulation indicated an immediate increase in CLK protein levels correlating with a
243 higher regulatory weight from *Clk* mRNA to protein, which mimics the effect of *Clk* uORF KO
244 (Fig. S4A). This, in turn, led to elevated levels of *per* and *tim* mRNA and protein (Fig. S4A and
245 S4B). In the simulations, we analyzed the intervals between peaks of *tim* mRNA, using these
246 as a measure of circadian period length. The mean ± SEM of period length is 23.926 ± 0.003
247 hours, 20.967 ± 0.078 hours, 18.956 ± 0.061 hours, and 17.494 ± 0.043 hours for regulatory
248 weights from *Clk* mRNA to CLK protein set at 0.026 (baseline), 0.027, 0.028, and 0.030,
249 respectively (Fig. 4B and 4C; SI Appendix, Table S2). These findings demonstrate a shortening
250 of the circadian period as the regulatory weight increases, suggesting that enhanced *Clk*
251 translation—resulting from the disruption of *Clk* uORFs—compresses the circadian period.
252
253 To corroborate the simulation outcomes, we measured the mRNA level of *per* and *tim*,
254 observing significant elevation in *Clk*-uORF-KO flies with the peak level occurring at an earlier
255 time in female heads (Fig. 4D). As our simulations predicted, disrupting *Clk* uORFs led to a
256 reduced period length by over one hour for the locomotor rhythm of *Clk*-uORF-KO flies.
257 Specifically, the period's mean ± SEM for WT males is 24.0 ± 0.25, WT females 24.2 ± 0.14,
258 *Clk*-uORF-KO males 22.8 ± 0.21, and *Clk*-uORF-KO females 22.7 ± 0.09 (Fig. 4E and 4F; SI
259 Appendix, Table S3). These empirical results, together with our simulation data, strongly
260 indicate that *Clk* uORFs modulate CLK translation, thereby regulating the timing of the
261 molecular clock through the expression of downstream genes like *per* and *tim*.
262
263 ***Clk* uORFs influence the temporal transcriptomic landscape**
264 CLK modulates the cyclical expression of a significant portion of *Drosophila* transcriptome [48].
265 To explore the impact of *Clk* uORFs on the global gene expression rhythms, we harvested heads
266 from WT and *Clk*-uORF-KO flies at four-hour intervals across the day, using three biological
267 replicates, and performed RNA sequencing for transcriptome analysis. Using JTK-CYCLE [49]
268 to detect genes with oscillating mRNA levels (Table S4), we found 3,370 and 3,859 genes
269 exhibited rhythmic expression in WT and *Clk*-uORF-KO female heads, respectively, with 2,235
270 genes in common (Fig. 5A and 5B). In male heads, 3,570 genes showed rhythmic expression

271 in WT, whereas 3,890 were rhythmic in *Clk*-uORF-KO, with 2,124 genes in common (Fig. 5C;
272 SI Appendix, Fig S5). Overall, knocking out *Clk* uORFs disrupted the rhythmic expression of
273 about 34-41% of genes in WT, while approximately 1,700 genes displayed *de novo* cyclic
274 expression patterns in *Clk*-uORF-KO heads. Gene ontology (GO) analysis demonstrated that
275 genes which lost rhythms in *Clk*-uORF-KO flies were mainly involved in rRNA processing,
276 ribosome biogenesis, translation and metabolism (SI Appendix, Fig. S6A and S6C), while genes
277 that gained rhythms when *Clk* uORFs were knocked out were enriched in pathways such as
278 translation, mitochondrial processes and development (SI Appendix, Fig. S6B and S6D).
279
280 Remarkably, genes related to circadian rhythms were significantly overrepresented
281 among rhythmically expressed genes in *Clk*-uORF-KO female heads (86 out of 150) compared
282 to the rest of the expressed genes (3,773 out of 9,051, Fisher's exact test, P = 0.02). This
283 enrichment was more significant in the heads of *Clk*-uORF-KO females than in WT females,
284 WT males, or *Clk*-uORF-KO males. Knocking out *Clk* uORFs led to an increase in oscillation
285 amplitude which was more significant in females than in males (Wilcoxon rank sum test; P =
286 5.72×10^{-9} in females vs. $P = 1.29\times10^{-5}$ in males; Fig. 5D and 5E). Furthermore, in females,
287 knocking out *Clk* uORFs led to desynchronized oscillations with peak expression time
288 distributed throughout the day (Fig. 5F and 5G). In summary, disrupting *Clk* uORFs markedly
289 influences gene expression rhythms in fly heads, exerting more pronounced effects in females
290 than males. These alterations in gene expression could result in diverse impacts on
291 physiological functions, especially in females, aspects of which are investigated in the
292 following sections.
293
294 ***Clk* uORFs promote morning wakefulness by tuning up the dopaminergic tone**
295 Building on evidence that CLK promotes sleep [50], we first examined the impact of knocking
296 out *Clk* uORFs on sleep. We found that knocking out *Clk* uORFs significantly lengthened sleep
297 duration, with more prominent alteration in females (9.5% increase; Fig. 6A; SI Appendix, Fig.
298 S7A) compared to males (4.0% increase; SI Appendix, Fig. S7B and S7C). A closer
299 examination showed that in female *Clk*-uORF-KO flies, the duration of sleep was notably
300 prolonged by 38.65% during the initial 8 hours of the light phase, indicating that *Clk* uORFs
301 facilitate morning wakefulness (Fig. 6B). The increase in sleep duration stems from a longer
302 average sleep bout, implicating enhanced sleep continuity upon *Clk* uORF deletion (Fig. 6C).
303 Additionally, waking activity levels were higher in female *Clk*-uORF-KO flies, indicating that
304 the prolonged sleep is not due to impaired motor function (Fig. 6C). While in males, the
305 alterations in sleep were not as prominent as that observed in females (SI Appendix, Fig. S7D).
306
307 Given that CLK suppresses expression of the gene encoding tyrosine hydroxylase (*ple*),

308 which in turn diminishes dopamine signaling and activity levels [51], we investigated whether
309 dopamine signaling mediates the influences of *Clk* uORFs on sleep. Our qPCR assays revealed
310 a notable decrease in *ple* mRNA in female *Clk*-uORF-KO heads compared to WT (Fig. 6D),
311 aligning with the hypothesis that elevated CLK protein levels—resulting from *Clk* uORF
312 disruption—downregulate *ple* expression. Next, we treated female flies with dopamine
313 precursor L-DOPA, which facilitates dopamine synthesis [52]. This treatment reversed the
314 prolonged sleep duration in female *Clk*-uORF-KO flies (Fig. 6E and 6F). Thus, *Clk* uORFs
315 appear to promote morning alertness by modulating dopaminergic signaling.
316
317 ***Clk* uORFs limit starvation-induced wakefulness and are beneficial for survival**
318 Starvation typically reduces sleep through a mechanism dependent on CLK, a response thought
319 to enhance survival chances [53]. To determine if *Clk* uORFs modulate the effects of starvation
320 on sleep/wakefulness, we analyzed sleep patterns in female *Clk*-uORF-KO flies during
321 starvation. We observed an exaggerated sleep loss in *Clk*-uORF-KO flies, suggesting that *Clk*
322 uORFs may function to restrict starvation-induced sleep loss (Fig. 6G-I). Moreover, the
323 increased wakefulness in *Clk*-uORF-KO flies correlated with significantly faster mortality rates
324 under starvation compared to WT flies for both sexes [$P = 8.8\times10^{-13}$ for females (Fig. 6J) and
325 $P = 2.4\times10^{-9}$ for males (SI Appendix, Fig. S8), log-rank test]. These results indicate that *Clk*
326 uORFs function to restrict sleep loss during starvation, which potentially affects survival.
327
328 ***Clk* uORFs modulate sleep/wakefulness in adaptation to seasonal photoperiodic changes**
329 **by suppressing CLK protein translation in a photoperiod-dependent manner**
330 Given the known significance of the circadian clock in adapting to seasonal environmental
331 variations [54], we hypothesized that *Clk* uORFs might similarly regulate translation on a
332 circannual basis. To test this hypothesis, we subjected female *Clk*-uORF-KO and WT flies to
333 conditions that mimic seasonal changes. Because the most important seasonal signal for the
334 circadian clock is the shortening/lengthening of photoperiod [54], we monitored locomotor
335 rhythm and sleep under photoperiods of different lengths, ranging from 4 hours of light and 20
336 hours of dark (4L20D) to 20 hours of light and 4 hours of dark (20L4D). Our observations
337 indicate that *Clk* uORFs did not influence the timing of locomotor activity rhythm across these
338 varied photoperiods, suggesting that *Clk* uORFs are not essential for adapting locomotor
339 rhythms to changes in seasonal day length (SI Appendix, Fig. S9).
340
341 Nevertheless, analysis of sleep duration under varying photoperiods revealed that female
342 *Clk*-uORF-KO flies exhibited a greater disparity from WT as the photoperiod decreased (Fig.
343 7A and 7B). Notably, sleep duration showed a significant positive correlation with photoperiod
344 length in WT (Pearson's $r = 0.323$, $P = 6.5 \times 10^{-8}$), while this correlation was much weaker in

345 *Clk*-uORF-KO (Pearson's $r = 0.172$, $P = 0.006$) (Fig. 7C). As the consequence, the difference
346 in sleep duration between *Clk*-uORF-KO and WT became larger as the photoperiod shortened
347 (Fig. 7B). Under 4L20D, the shortest photoperiod tested here, WT displayed on average 918 ±
348 26 minutes of sleep, while that of *Clk*-uORF-KO females was 1,124 ± 18 minutes, with an
349 increase of 206 minutes on average (22.44%). In contrast, under 20L4D, the longest
350 photoperiod tested, WT females slept for 1,082 ± 21 minutes compared to 1,195 ± 18 minutes
351 for *Clk*-uORF-KO females, yielding a smaller difference of 113 minutes on average (10.44%).
352 These findings indicate that *Clk*-uORF-KO flies showed a diminished response to changes in
353 photoperiod length, implying that *Clk* uORF-mediated translational regulation plays a role in
354 synchronizing sleep patterns with seasonal daylight variations.
355
356 Given these observed behavioral changes, we posited that *Clk* uORFs participate in
357 translational regulation in a photoperiod-dependent manner. To test this, we carried out
358 ribosome fractionation followed by qPCR under 4L20D and 12L12D light-dark cycles. In WT
359 heads, we observed a consistent decrease in P-to-M ratios throughout the day under 12L12D
360 vs. 4L20D (Fig. 8A). However, such a pattern was not observed in *Clk*-uORF-KO (Fig. 8B).
361 The area under the curve (AUC) of these ratios, indicative of overall daily CLK protein
362 synthesis, was significantly reduced by long photoperiods in WT fly heads (~30% reduction),
363 while the reduction was much less (~8% reduction) in *Clk*-uORF-KO (Fig. 8C and 8D). This
364 photoperiod dependency was corroborated at the protein level. In WT heads, CLK protein levels
365 dipped significantly during ZT4-12 under 4L20D compared to 12L12D (Fig. 8E and 8F). In
366 contrast, CLK protein level was only significantly decreased at ZT0 in *Clk*-uORF-KO under
367 4L20D relative to 12L12D (Fig. 8E and 8F). Moreover, the AUC analysis demonstrated that
368 short photoperiod significantly reduced total daily CLK level in WT but not in *Clk*-uORF-KO
369 heads (SI Appendix, Fig. S10). Collectively, these findings suggest that *Clk* uORFs are involved
370 in photoperiod-dependent translation suppression, which likely aids in adjusting wakefulness
371 to seasonal variations.
372
373 **Knocking out *Clk* uORFs impairs fecundity**
374 Recognizing the roles of *Clk* uORFs in facilitating the adaptation to environmental changes, we
375 further investigated whether they enhance evolutionary fitness by assessing fecundity.
376 Remarkably, mated *Clk*-uORF-KO females laid significantly fewer eggs than their WT
377 counterparts during an eight-day monitoring duration, with the total egg production of mutants
378 markedly less ($P < 0.01$) (SI Appendix, Fig. S11A). This pattern persisted in *Clk*-uORF-KO
379 virgin females, which also laid fewer eggs than WT in both segmented (2-days) and pooled
380 (10-days) measurements (SI Appendix, Fig. S11B). Accordingly, female *Clk*-uORF-KO flies
381 produced significantly fewer offspring than WT counterparts at 25°C ($P = 1.5\times10^{-5}$ Wilcoxon

rank sum test) (SI Appendix, Fig. S11C). Even at 29°C, when both mutants and WT flies exhibited reduced offspring production compared to 25°C, the offspring counts for *Clk*-uORF-KO females were still significantly fewer than that for WT (P = 0.00029, Wilcoxon rank sum test) (SI Appendix, Fig. S11C). Collectively, these results indicate that *Clk* uORFs profoundly affect various aspects of physiological and behavioral processes, with implications for fitness beyond their established roles in circadian rhythm and sleep regulation.

Discussion

The evolutionary conservation of the circadian mechanisms across species underscores their fundamental significance. Our understanding of circadian rhythms has grown substantially over the years, providing critical insights into a range of physiological processes. Earlier investigations, including our own, have noted a very low correlation between the temporal variation pattern of the transcriptome and that of the proteome, indicating that regulations at the translational and post-translational levels play dominant roles in determining the daily variations of protein abundance [55]. Within this complex regulatory network, our study here has highlighted a pivotal role for translational regulation, specifically mediated by uORFs, in fine-tuning these rhythms. Beyond circadian rhythm and sleep, *Clk*-uORF-KO flies show diminished fecundity and reduced starvation resilience, suggesting that *Clk* uORFs might act as a master regulator, shaping the rhythmic expression of a vast array of genes and influencing multifaceted physiological outcomes.

In this study, we observed over one-hour shortening of the circadian period when *Clk* uORFs were knocked out, which means these uORFs play a crucial role in the core circadian timing mechanism. Consistent with this idea, we found that *Clk* uORFs mediate an instructive signal to the molecular clock by suppressing CLK protein translation during the daytime. Besides setting the pace of the clock, *Clk* uORFs also modulate cyclic gene expression globally. The oscillation of over 1/3 of the rhythmic genes requires *Clk* uORFs, as these oscillations were dampened in *Clk*-uORF-KO flies. This reveals the delicacy of the circadian system: an increase of CLK translation and, thus, CLK protein level caused by knocking out *Clk* uORFs can exert detrimental effects on the rhythmicity of the transcriptome. It is surprising that genes cycle with a more robust amplitude in *Clk*-uORF-KO flies relative to WT. Among these genes, about half did not display oscillatory expression patterns in WT. In other words, *Clk* uORFs suppress the mRNA rhythms of these genes. We reason that knocking out *Clk* uORFs increases CLK protein level in a time-dependent manner, which results in enhanced transcription of CLK target genes at a certain time of the day, and thus, these genes may acquire a *de novo* rhythmic expression pattern. Considering that *Clk* uORFs suppress CLK translation more under longer photoperiods and less under shorter photoperiods, we speculate this photoperiod-dependent variation in the

translational activities of *Clk* uORFs can shape the rhythmic transcription landscape in adaptation to seasonal photoperiod changes.

Clk uORFs promote morning wakefulness, consistent with the time-dependent modulation of these uORFs on CLK protein translation and abundance. This regulation is not only time of the day-dependent, but also time of the year-dependent. WT flies display increased wakefulness and decreased sleep in adaptation to a shortening of photoperiod (occurring in fall and winter seasons), while *Clk* uORFs participate in modulating this process by suppressing CLK translation in a photoperiod-dependent manner. Intriguingly, human individuals with seasonal affective disorder (SAD, commonly known as winter depression) report a winter increase in sleep, ranging from 30 min to 2 h longer in duration compared to controls, while the underlying mechanism is yet unknown [56]. The long sleep phenotype caused by knocking out *Clk* uORFs is most striking under a short photoperiod, reminiscent of the winter hypersomnolence in SAD. Notably, while we observed a stronger sleep phenotype in female flies, SAD is also more predominant in women [57]. From a mechanistic perspective, our results strongly suggest that *Clk* uORFs promote wakefulness by increasing tyrosine hydroxylase expression, thus up-regulating the dopaminergic tone. Similarly, the mammalian CLOCK protein has been shown to repress the transcription of *Tyrosine hydroxylase*, while *Clock* mutation leads to decreased sleep and depression-like behaviors in mice due to elevated dopamine signaling [58,59]. Taken together, our findings here may provide some insights for understanding the pathological mechanism of SAD.

It seems contradictory that CLK translation is down-regulated under 12L12D vs. 4L20D, while CLK protein level is higher under 12L12D relative to 4L20D. We reason that CLK protein abundance is determined by coordinated actions of transcription, translation, and post-translational modifications. A longer photoperiod may promote transcription and/or inhibit degradation of CLK protein, while *Clk* uORFs counteract these influences by suppressing CLK synthesis. In other words, *Clk* uORFs may serve as a buffer against the impacts of transcription and/or PTMs, adjusting CLK protein abundance to maintain an optimal level throughout the year. Of course, further investigations are needed to elucidate how *Clk* uORFs mediate photoperiodic signals.

uORFs have been shown to dynamically modulate the translation of CDSs in stress responses [30] , and here we also observed a role for *Clk* uORFs in responses to starvation stress. Although under food *ad libitum* condition, *Clk* uORFs promote wakefulness, under starvation they function to reduce wakefulness, implicating the complexity of uORF regulation and their multifaceted roles in varying physiological states. Despite these complicated and sometimes contradictory actions, in the end, the presence of *Clk* uORFs confers adaptive advantages and

is beneficial for the survival (KO flies die earlier when starved) and fecundity of the organism.

To summarize, here we observed an enrichment of uORFs in circadian rhythm genes and further identified functional uORFs in *Clk* that repress the translation of CLK protein in both circadian and circannual manners. These regulations slow down the pace of the clock, modulate global rhythms of gene expression, and promote morning wakefulness in adaption to seasonal photoperiod changes. These findings, situated within the broader evolutionary, clinical, and interdisciplinary contexts, underscore the pivotal role of uORFs in shaping biological processes and potential therapeutic avenues.

Acknowledgements

This work was supported by grants from the Natural Science Foundation of China (31930021 and 32341021 to L.Z., 32070597 to J. L, and 32200956 to K.S.), the Ministry of Science and Technology of China (STI 2030-Major Projects 2021ZD0203200-02 to L.Z, and 2022YFE0132000 to J.L.), the Department of Science and Technology of Hubei Province (2022CFA049 to L.Z.) and Natural Science Foundation of Beijing (grant 5212006 to J.L.). We thank the National Center for Protein Sciences at Peking University for technical assistance. Some of the analyses were performed on the High-Performance Computing Platform of the Center for Life Sciences. We thank Dr. Joanna Chiu for CLK antibody used in this study.

Data and code availability

- The raw fastq files for the RNA-seq libraries were deposited to NCBI Sequence Read Archive (SRA) with BioProject accession PRJNA1026336 and are publicly available as of the date of publication.
- Original Western blot images have been deposited to Mendeley and are publicly available on the date of publication.
- Any additional information required to reanalyze the data reported in this paper is available from the lead contact upon request.
-

References

1. Li, S., and Zhang, L. (2015). Circadian Control of Global Transcription. Biomed Res Int *2015*, 187809. 10.1155/2015/187809.
2. Dunlap, J.C. (1999). Molecular bases for circadian clocks. Cell *96*, 271-290. 10.1016/s0092-8674(00)80566-8.
3. Patke, A., Young, M.W., and Axelrod, S. (2020). Molecular mechanisms and physiological importance of circadian rhythms. Nature Reviews Molecular Cell Biology *21*, 67-84. 10.1038/s41580-019-0179-2.
4. Panda, S., Hogenesch, J.B., and Kay, S.A. (2002). Circadian rhythms from flies to

494 human. Nature *417*, 329-335. 10.1038/417329a.
495 5. Takahashi, J.S. (2017). Transcriptional architecture of the mammalian circadian clock.
496 Nature Reviews Genetics *18*, 164-179. 10.1038/nrg.2016.150.
497 6. Reinke, H., and Asher, G. (2019). Crosstalk between metabolism and circadian clocks.
498 Nature Reviews Molecular Cell Biology *20*, 227-241. 10.1038/s41580-018-0096-9.
499 7. Masri, S., and Sassone-Corsi, P. (2013). The circadian clock: a framework linking
500 metabolism, epigenetics and neuronal function. Nat Rev Neurosci *14*, 69-75.
501 10.1038/nrn3393.
502 8. Palm, D., Uzoni, A., Simon, F., Fischer, M., Coogan, A., Tucha, O., Thome, J., and
503 Faltraco, F. (2021). Evolutionary conservations, changes of circadian rhythms and their
504 effect on circadian disturbances and therapeutic approaches. Neurosci Biobehav Rev
505 *128*, 21-34. 10.1016/j.neubiorev.2021.06.007.
506 9. Rosbash, M. (2009). The Implications of Multiple Circadian Clock Origins. PLOS
507 Biology *7*, e1000062. 10.1371/journal.pbio.1000062.
508 10. Young, M.W., and Kay, S.A. (2001). Time zones: a comparative genetics of circadian
509 clocks. Nat Rev Genet *2*, 702-715. 10.1038/35088576.
510 11. Tataroglu, O., and Emery, P. (2014). Studying circadian rhythms in Drosophila
511 melanogaster. Methods *68*, 140-150. https://doi.org/10.1016/j.ymeth.2014.01.001.
512 12. Rosato, E., Tauber, E., and Kyriacou, C.P. (2006). Molecular genetics of the fruit-fly
513 circadian clock. European Journal of Human Genetics *14*, 729-738.
514 10.1038/sj.ejhg.5201547.
515 13. Dubowy, C., and Sehgal, A. (2017). Circadian Rhythms and Sleep in Drosophila
516 melanogaster. Genetics *205*, 1373-1397. 10.1534/genetics.115.185157.
517 14. Zehring, W.A., Wheeler, D.A., Reddy, P., Konopka, R.J., Kyriacou, C.P., Rosbash, M.,
518 and Hall, J.C. (1984). P-element transformation with period locus DNA restores
519 rhythmicity to mutant, arrhythmic Drosophila melanogaster. Cell *39*, 369-376.
520 10.1016/0092-8674(84)90015-1.
521 15. Allada, R., White, N.E., So, W.V., Hall, J.C., and Rosbash, M. (1998). A mutant
522 Drosophila homolog of mammalian Clock disrupts circadian rhythms and transcription
523 of period and timeless. Cell *93*.
524 16. Rutila, J.E. (1998). CYCLE is a second bHLH–PAS clock protein essential for
525 circadian rhythmicity and transcription of Drosophila period and timeless. Cell *93*.
526 17. Sehgal, A., Price, J.L., Man, B., and Young, M.W. (1994). Loss of circadian behavioral
527 rhythms and per RNA oscillations in the Drosophila mutant timeless. Science *263*.
528 18. Kadener, S., Menet, J.S., Schoer, R., and Rosbash, M. (2008). Circadian transcription
529 contributes to core period determination in Drosophila. PLOS Biol. *6*.
530 19. Zhao, J. (2003). Drosophila clock can generate ectopic circadian clocks. Cell *113*.
531 20. Lee, J., Yoo, E., Lee, H., Park, K., Hur, J.H., and Lim, C. (2017). LSM12 and
532 ME31B/DDX6 Define Distinct Modes of Posttranscriptional Regulation by ATAXIN-
533 2 Protein Complex in Drosophila Circadian Pacemaker Neurons. Mol Cell *66*, 129-140
534 e127. 10.1016/j.molcel.2017.03.004.
535 21. Lim, C., and Allada, R. (2013). ATAXIN-2 activates PERIOD translation to sustain
536 circadian rhythms in Drosophila. Science *340*, 875-879. 10.1126/science.1234785.
537 22. Lim, C., Lee, J., Choi, C., Kilman, V.L., Kim, J., Park, S.M., Jang, S.K., Allada, R.,

538 and Choe, J. (2011). The novel gene twenty-four defines a critical translational step in
539 the Drosophila clock. Nature *470*, 399-403. 10.1038/nature09728.
540 23. Zhang, Y., Ling, J., Yuan, C., Dubruille, R., and Emery, P. (2013). A role for Drosophila
541 ATX2 in activation of PER translation and circadian behavior. Science *340*, 879-882.
542 10.1126/science.1234746.
543 24. Kadener, S. (2009). A role for microRNAs in the Drosophila circadian clock. Genes
544 Dev. *23*.
545 25. Chen, X., and Rosbash, M. (2016). mir-276a strengthens Drosophila circadian rhythms
546 by regulating timeless expression. Proc. Natl Acad. Sci. USA *113*.
547 26. Chen, W. (2014). Regulation of Drosophila circadian rhythms by miRNA let-7 is
548 mediated by a regulatory cycle. Nat. Commun. *5*.
549 27. Zhang, H., Wang, Y., Wu, X., Tang, X., Wu, C., and Lu, J. (2021). Determinants of
550 genome-wide distribution and evolution of uORFs in eukaryotes. Nature
551 Communications *12*, 1076. 10.1038/s41467-021-21394-y.
552 28. Hinnebusch, A.G., Ivanov, I.P., and Sonenberg, N. (2016). Translational control by 5'-
553 untranslated regions of eukaryotic mRNAs. Science *352*, 1413-1416.
554 10.1126/science.aad9868.
555 29. Morris, D.R., and Geballe, A.P. (2000). Upstream open reading frames as regulators of
556 mRNA translation. Mol Cell Biol *20*, 8635-8642. 10.1128/MCB.20.23.8635-
557 8642.2000.
558 30. Zhang, H., Wang, Y., and Lu, J. (2019). Function and Evolution of Upstream ORFs in
559 Eukaryotes. Trends Biochem Sci *44*, 782-794. 10.1016/j.tibs.2019.03.002.
560 31. Barbosa, C., Peixeiro, I., and Romão, L. (2013). Gene expression regulation by
561 upstream open reading frames and human disease. PLoS Genet *9*, e1003529.
562 10.1371/journal.pgen.1003529.
563 32. Ruiz-Orera, J., and Alba, M.M. (2019). Translation of Small Open Reading Frames:
564 Roles in Regulation and Evolutionary Innovation. Trends Genet *35*, 186-198.
565 10.1016/j.tig.2018.12.003.
566 33. Diernfellner, A.C., Schafmeier, T., Merrow, M.W., and Brunner, M. (2005). Molecular
567 mechanism of temperature sensing by the circadian clock of Neurospora crassa. Genes
568 Dev *19*, 1968-1973. 10.1101/gad.345905.
569 34. Wu, H.W., Fajiculay, E., Wu, J.F., Yan, C.S., Hsu, C.P., and Wu, S.H. (2022). Noise
570 reduction by upstream open reading frames. Nat Plants *8*, 474-480. 10.1038/s41477-
571 022-01136-8.
572 35. Montenegro-Montero, A., Canessa, P., and Larrondo, L.F. (2015). Around the Fungal
573 Clock: Recent Advances in the Molecular Study of Circadian Clocks in Neurospora
574 and Other Fungi. Adv Genet *92*, 107-184. 10.1016/bs.adgen.2015.09.003.
575 36. Salichos, L., and Rokas, A. (2010). The diversity and evolution of circadian clock
576 proteins in fungi. Mycologia *102*, 269-278. 10.3852/09-073.
577 37. Jabbur, M.L., and Johnson, C.H. (2022). Spectres of Clock Evolution: Past, Present,
578 and Yet to Come. Frontiers in Physiology *12*. 10.3389/fphys.2021.815847.
579 38. Miyake, T., Inoue, Y., Shao, X., Seta, T., Aoki, Y., Nguyen Pham, K.T., Shichino, Y.,
580 Sasaki, J., Sasaki, T., Ikawa, M., et al. (2023). Minimal upstream open reading frame
581 of Per2 mediates phase fitness of the circadian clock to day/night physiological body

temperature rhythm. Cell Rep *42*, 112157. 10.1016/j.celrep.2023.112157.

39. Millius, A., Yamada, R.G., Fujishima, H., Maeda, K., Standley, D.M., Sumiyama, K., Perrin, D., and Ueda, H.R. (2023). Circadian ribosome profiling reveals a role for the Period2 upstream open reading frame in sleep. Proc Natl Acad Sci U S A *120*, e2214636120. 10.1073/pnas.2214636120.

40. Jang, C., Lahens, N.F., Hogenesch, J.B., and Sehgal, A. (2015). Ribosome profiling reveals an important role for translational control in circadian gene expression. Genome Res *25*, 1836-1847. 10.1101/gr.191296.115.

41. Janich, P., Arpat, A.B., Castelo-Szekely, V., Lopes, M., and Gatfield, D. (2015). Ribosome profiling reveals the rhythmic liver translatome and circadian clock regulation by upstream open reading frames. Genome Res *25*, 1848-1859. 10.1101/gr.195404.115.

42. Zhang, H., Dou, S., He, F., Luo, J., Wei, L., and Lu, J. (2018). Genome-wide maps of ribosomal occupancy provide insights into adaptive evolution and regulatory roles of uORFs during Drosophila development. PLoS Biol *16*, e2003903. 10.1371/journal.pbio.2003903.

43. Zhang, H., Wang, Y., Wu, X., Tang, X., Wu, C., and Lu, J. (2021). Determinants of genome-wide distribution and evolution of uORFs in eukaryotes. Nat Commun *12*, 1076. 10.1038/s41467-021-21394-y.

44. Abdelmohsen, K., Panda, A.C., Kang, M.J., Guo, R., Kim, J., Grammatikakis, I., Yoon, J.H., Dudekula, D.B., Noh, J.H., Yang, X., et al. (2014). 7SL RNA represses p53 translation by competing with HuR. Nucleic Acids Res *42*, 10099-10111. 10.1093/nar/gku686.

45. Panda, A.C., Abdelmohsen, K., Martindale, J.L., Di Germanio, C., Yang, X., Grammatikakis, I., Noh, J.H., Zhang, Y., Lehrmann, E., Dudekula, D.B., et al. (2016). Novel RNA-binding activity of MYF5 enhances Ccnd1/Cyclin D1 mRNA translation during myogenesis. Nucleic Acids Res *44*, 2393-2408. 10.1093/nar/gkw023.

46. Panda, A.C., Martindale, J.L., and Gorospe, M. (2017). Polysome Fractionation to Analyze mRNA Distribution Profiles. Bio Protoc *7*. 10.21769/BioProtoc.2126.

47. Fathallah-Shaykh, H.M., Bona, J.L., and Kadener, S. (2009). Mathematical model of the Drosophila circadian clock: loop regulation and transcriptional integration. Biophys J *97*, 2399-2408. 10.1016/j.bpj.2009.08.018.

48. Abruzzi, K.C., Rodriguez, J., Menet, J.S., Desrochers, J., Zadina, A., Luo, W., Tkachev, S., and Rosbash, M. (2011). Drosophila CLOCK target gene characterization: implications for circadian tissue-specific gene expression. Genes Dev *25*, 2374-2386. 10.1101/gad.178079.111.

49. Hughes, M.E., Hogenesch, J.B., and Kornacker, K. (2010). JTK_CYCLE: an efficient nonparametric algorithm for detecting rhythmic components in genome-scale data sets. J Biol Rhythms *25*, 372-380. 10.1177/0748730410379711.

50. Liu, S., Lamaze, A., Liu, Q., Tabuchi, M., Yang, Y., Fowler, M., Bharadwaj, R., Zhang, J., Bedont, J., Blackshaw, S., et al. (2014). WIDE AWAKE mediates the circadian timing of sleep onset. Neuron *82*, 151-166. 10.1016/j.neuron.2014.01.040.

51. Kumar, S., Chen, D., and Sehgal, A. (2012). Dopamine acts through Cryptochrome to promote acute arousal in Drosophila. Genes Dev *26*, 1224-1234.

10.1101/gad.186338.111.

52. Pendleton, R.G., Rasheed, A., Paluru, P., Joyner, J., Jerome, N., Meyers, R.D., and Hillman, R. (2005). A developmental role for catecholamines in Drosophila behavior. Pharmacol Biochem Behav *81*, 849-853. 10.1016/j.pbb.2005.06.008.

53. Keene, A.C., Duboue, E.R., McDonald, D.M., Dus, M., Suh, G.S., Waddell, S., and Blau, J. (2010). Clock and cycle limit starvation-induced sleep loss in Drosophila. Curr Biol *20*, 1209-1215. 10.1016/j.cub.2010.05.029.

54. Wood, S., and Loudon, A. (2014). Clocks for all seasons: unwinding the roles and mechanisms of circadian and interval timers in the hypothalamus and pituitary. J Endocrinol *222*, R39-59. 10.1530/JOE-14-0141.

55. Wang, C., Shui, K., Ma, S., Lin, S., Zhang, Y., Wen, B., Deng, W., Xu, H., Hu, H., Guo, A., et al. (2020). Integrated omics in Drosophila uncover a circadian kinome. Nat Commun *11*, 2710. 10.1038/s41467-020-16514-z.

56. Wescott, D.L., Soehner, A.M., and Roecklein, K.A. (2020). Sleep in seasonal affective disorder. Curr Opin Psychol *34*, 7-11. 10.1016/j.copsyc.2019.08.023.

57. Jepson, T.L., Ernst, M.E., and Kelly, M.W. (1999). Current Perspectives on the Management of Seasonal Affective Disorder. Journal of the American Pharmaceutical Association (1996) *39*, 822-829. 10.1016/s1086-5802(15)30373-9.

58. Roybal, K., Theobold, D., Graham, A., DiNieri, J.A., Russo, S.J., Krishnan, V., Chakravarty, S., Peevey, J., Oehrlein, N., Birnbaum, S., et al. (2007). Mania-like behavior induced by disruption of CLOCK. Proc Natl Acad Sci U S A *104*, 6406-6411. 10.1073/pnas.0609625104.

59. Sidor, M.M., Spencer, S.M., Dzirasa, K., Parekh, P.K., Tye, K.M., Warden, M.R., Arey, R.N., Enwright, J.F., Jacobsen, J.P., Kumar, S., et al. (2015). Daytime spikes in dopaminergic activity drive rapid mood-cycling in mice. Mol Psychiatry *20*, 1479-1480. 10.1038/mp.2015.8.

60. Sisobhan, S., Rosensweig, C., Lear, B.C., and Allada, R. (2022). SleepMat: a new behavioral analysis software program for sleep and circadian rhythms. Sleep *45*. 10.1093/sleep/zsac195.

61. Dobin, A., Davis, C.A., Schlesinger, F., Drenkow, J., Zaleski, C., Jha, S., Batut, P., Chaisson, M., and Gingeras, T.R. (2013). STAR: ultrafast universal RNA-seq aligner. Bioinformatics *29*, 15-21.

62. Anders, S., Pyl, P.T., and Huber, W. (2015). HTSeq--a Python framework to work with high-throughput sequencing data. Bioinformatics *31*, 166-169. 10.1093/bioinformatics/btu638.

63. Gene Ontology, C. (2021). The Gene Ontology resource: enriching a GOld mine. Nucleic Acids Res *49*, D325-D334. 10.1093/nar/gkaa1113.

665 **Materials and Methods**

666

667 **Fly strains and cell line**

668 All flies were reared on standard cornmeal-yeast-sucrose medium and kept in light/dark (LD)
669 cycles at 25°C except for specific experimental design denoted in the text. Food was accessible
670 *ad libitum*. *{nos-Cas9}attP40* and *{nos-Cas9}attP2* fly stocks used for embryo injection were
671 from the TsingHua Fly Center. The tool fly stocks (*y sc v* and *Dr, e/TM3, Sb*) used for mutant
672 screening were from the TsingHua Fly Center. *Clk*-uORF-KO and *cyc*-uORF-KO mutants were
673 generated and backcrossed to the Canton-S strain for nine generations. Homozygous mutants
674 were used throughout this study and the Canton-S strain served as the WT control flies.
675 *Drosophila* S2 cells used in this study were purchased from Life Technologies Corp
676 (http://www.lifetechnologies.com).

677

678 **The conservation assessment of uORFs**

679 We retrieved the whole genome sequence alignment (maf) of *D. melanogaster* (dm6) with 22
680 other *Drosophila* species from the UCSC genome browser (genome.ucsc.edu). Leveraging the
681 genome annotation of *D. melanogaster* (FlyBase r6.04, https://flybase.org/), the 5'UTR
682 sequence of each annotated transcript of *D. melanogaster* and its corresponding sequences in
683 other 22 *Drosophila* were extracted from the maf. We scanned all the AUG triplets within the
684 5'UTRs of *D. melanogaster* and then determined their presence or absence in the corresponding
685 positions in the other species based on maf. AUG triplets that overlapped with any annotated
686 CDS region were removed. The transcriptome and translatome data was obtained from the
687 previous study [42].

688

689 **Generation of uORF-KO strain**

690 We searched for possible sgRNA target sites near the start codon of the uORFs of *Clk* and *cyc*
691 genes using the Benchling website (https://www.benchling.com/crispr/) to design optimal
692 single guide RNA (sgRNA) sequences with high specificity and low off-target effects. Two
693 pairs of sgRNAs were used for each gene. We then synthesized single-stranded complementary
694 DNAs (ssDNAs) and annealed them to obtain double-stranded DNA (dsDNA), which served
695 as the template for sgRNA expression. The dsDNA was then ligated into the BbsI-digested
696 pU6B vector. The template sequences of the sgRNA uATG-KO are listed in SI Appendix, Table
697 S5. The screening procedures of mutant flies are provided in the (SI Appendix, SI Methods).

698

699 **uORF mutation sequencing validation**

700 The mutant fly was homogenized with DNA sequencing extract buffer [10 mM Tris-HCl at pH
701 8.0, 1 mM EDTA at pH 8.0, 25 mM NaCl and 0.02 % proteinase K (CW2584, CWBIO)] and

702 incubated at 37°C for 30 min. PCR was performed with Taq Plus MasterMix (CW2849,
703 CWbiotech). The PCR reaction was performed as follows: 94 °C for 2 min followed by 94 °C
704 for 10 s, 57°C for 15 s, and 72°C for 1 min 20 s for 35 cycles. The primers used were listed in
705 (SI Appendix, Table S5). PCR products were sequenced using commercial Sanger sequencing
706 (AuGCT Co.).
707
708 **Cell culture and transfection**
709 S2 cells were cultured in Schneider's *Drosophila* Medium (Sigma) containing 10% heat-
710 inactivated fetal bovine serum (FBS), 100 U/ml penicillin, and 100 μg/ml streptomycin
711 (Thermo Fisher) at 25°C for 24 h to reach 2-4 × 10^6 cells/ml before further treatments. Plasmid
712 transfection was conducted with Lipofectamine 3000 (L3000001, Thermo Fisher) according to
713 the supplier's protocol.
714
715 **Dual-luciferase assay**
716 The wild-type (WT) 5'UTR of *Clk* and *cyc* was cloned from cDNA by PCR, and uATG
717 mutations were introduced into 5'UTR by the amplification primers. The PCR primers used for
718 this purpose are listed in (SI Appendix, Table S5). The WT and mutated 5'UTR sequences were
719 ligated into a linearized reporter plasmid (psiCHECK-2 vector, Promega). The entire sequences
720 of all the plasmids were validated by Sanger sequencing. The *Renilla* luciferase activity
721 associated with WT or uORF-mutated 5'UTRs was measured according to the manual of the
722 Dual-Luciferase Reporter Assay System (Promega) 32 h after transfection and was normalized
723 to the activity of firefly luciferase.
724
725 **Fly head collection**
726 Flies were collected within 3-7 days of eclosion and entrained in LD for three days. After that,
727 they were transferred into constant darkness (DD). Flies were collected during LD or on the
728 first day of DD and frozen at -80°C. Frozen flies were vortexed for 10 s to separate the head
729 from the body.
730
731 **Ribosome fraction analysis**
732 The heads obtained from WT and mutant flies were collected and homogenized with lysis buffer,
733 the lysates were clarified by centrifugation at 4°C and 20,000×g for 10 min, and the
734 supernatants were applied to sucrose gradient ultracentrifugation. For each sample, the ratio of
735 *Clk* and *cyc* mRNA abundance in the polysome fraction to that in the monosome fraction was
736 calculated as the P-to-M ratio. Six biological replicates were performed for each sample. Details
737 of the procedures can be found in the (SI Appendix, SI Methods).
738

739 **Western blot**

740 Proteins were extracted from fly heads and cultured cells using SDS lysis buffer [50 mM Tris-
741 HCl at pH 7.6, 150 mM NaCl, 1% Triton X-100, 0.5% SDS, 1 mM EDTA at pH8.0, 2 mM DTT,
742 1 × proteinase inhibitor and phosphatase inhibitor (4693116001 and 04906845001, Roche)].
743 After homogenization, protein lysates were centrifuged at 12,000 × *g* for 15 min at 4°C and
744 incubated at 95°C in the loading buffer for 5 min. Equal amounts of protein were loaded into
745 each well on 6% SDS-PAGE gels and then transferred to nitrocellulose membranes for 2 h at
746 90 V. Membranes were incubated with primary antibody at 4°C overnight, followed by
747 secondary antibody at room temperature for 1 h. The primary antibodies used were as follows:
748 guinea pig anti-CLK (1:1000, gift from Dr. Joanna Chiu) and rabbit anti-ACTIN 57B (1:5000,
749 AC026, ABclonal, CN). Donkey secondary antibodies (1:10000 dilution) were conjugated
750 either with IRDye 680 or IRDye 800 (926-68072 and 926-32213, LI-COR Biosciences, US).
751 Bands were visualized and quantified with an Odyssey Infrared Imaging System (LI-COR
752 Biosciences).

753

754 **Model simulation for the outcome of enhanced *Clk* translation**

755 We adopted a previously published mathematical model of the *Drosophila* circadian clock [47].
756 This system relies on a nonlinear, autonomous, first-order system of ordinary differential
757 equations to simulate the regulatory weights among mRNAs or protein molecules in the
758 molecular clock network. Details of the simulation can be found in the (SI Appendix, SI
759 Methods).

760

761 **Total RNA extraction and RT-qPCR**

762 RNA was extracted from frozen fly heads maintained at -80°C. 50 fly heads per sample were
763 homogenized in Total RNA Isolation (TRIzol) Reagent (15596026, Invitrogen) by using a
764 homogenizer with plastic beads. After mixing with trichloromethane, homogenates were
765 centrifuged at 12,000 × *g* and the suspension was precipitated with 75% ethanol. After air dry,
766 total RNA was reverse-transcribed into cDNA and genomic DNA was removed with One-step
767 cDNA Synthesis SuperMix (AT311, Transgen). Quantitative real-time PCR was performed with
768 One-Step RT-PCR SuperMix (AT141, Transgen). The PCR reaction was performed as follows:
769 45°C for 5 min; 94°C for 2 min; 94°C for 5 s, 60°C for 15 s, 72°C for 20 s for 40 cycles (Applied
770 Biosystems). The ΔΔCT method was used for quantification. *Beta-Actin* was used as an internal
771 control. The primers used are listed in (SI Appendix, Table S5).

772

773 **Locomotor activity monitoring and analysis**

774 Locomotor activity levels of adult flies were monitored by *Drosophila* Activity Monitoring
775 System (TriKinetics) for 7 days of LD followed by 7 days of DD. For DD rhythmicity, chi-

776 squared periodogram analyses were performed by Clocklab (Actimetrics). Rhythmic flies were
777 defined as those in which the chi-squared power was ≥ 10 above the significance line. Period
778 calculations considered only rhythmic flies. Dead flies were defined by 0 activity on DD7 and
779 removed from the analysis.
780
781 **Sleep measurement and analysis**
782 *Drosophila* Activity Monitor system (Trikinetics) was used to analyze fly sleep. Virgin female
783 and male flies of 3~5 days old were used for the experiments unless otherwise specified. Flies
784 were entrained under LD at 25°C for 3 days, and then their activities in the next 3 days under
785 LD conditions were analyzed.
786 For sleep analysis during starvation, 3~5 days old virgin females were used. After 3 days
787 of entrainment in monitoring tubes with standard media (2% agar and 5% sucrose), baseline
788 sleep was measured for 2 days. Standard food was then replaced at ZT0 by starvation media
789 (2% agar) for 24 h. Flies were then re-fed with standard media for an additional 24-hour
790 recovery period.
791 Sleep is defined as 5 min consecutive inactivity. Sleep was analyzed with SleepMat
792 following previously published protocol [60].
793
794 **RNA-seq and circadian analysis**
795 We collected heads from *Clk*-uORF-KO mutants and WT flies raised under LD cycles at 25°C
796 at ZT 0, 4, 8, 12, 16 and 20. Library construction and sequencing with PE150 were conducted
797 by Annoroad on the Illumina Nova6000 platform. Three biological replicates were sequenced
798 for each sample. The clean data were mapped to the reference genome of *D. melanogaster*
799 (FlyBase, r6.04) using STAR [61]. Reads mapped to the exons of each gene were tabulated with
800 htseq-count [62]. Rhythmically expressed genes were identified by JTK_CYCLE under the
801 threshold of < 0.05 on the permutation-based *P* values of the Jonckheere-Terpstra test (ADJ.P)
802 implemented in the JTK CYCLE.
803
804 **GO-based enrichment**
805 For GO-based enrichment analysis, GO annotation files were downloaded on 15 November
806 2023 from the Gene Ontology Resource (http://geneontology.org/)[63] and contained 14,736 fly
807 genes with at least one GO term. For each GO term *t*, we defined the following:
808 N = the total number of genes in the background distribution.
809 n = the total number of genes for GO analysis.
810 M = the total number of genes annotated by GO term t.
811 m = the number of genes annotated by GO term t in n.
812 The enrichment ratio (E-ratio) of t was then computed, and the P was calculated with the

hypergeometric distribution as follows:

$$\mathrm{E-ratio} = \frac{m}{M}/\frac{n}{N} \tag{1}$$

$$P = \sum_{m'=m}^{n} \frac{\binom{M}{m'}\binom{N-M}{n-m'}}{\binom{N}{n}} (\mathrm{E-ratio} \geq 1), \mathrm{or} \tag{2}$$

$$P = \sum_{m'=0}^{m} \frac{\binom{M}{m'}\binom{N-M}{n-m'}}{\binom{N}{n}} (\mathrm{E-ratio} < 1) \tag{3}$$

Drug treatment

For pharmacological experiments, 5 mg/ml L-DOPA (BBI Life Sciences) was mixed in the fly food, and the flies were fed with L-Dopa food during sleep monitoring.

Egg numbers quantification

Newly hatched virgins were picked out and allowed to mature for two days in separate vials. They were then mated by placing one virgin female with three male flies for two days. Subsequently, ten female parents from each group were transferred to a fresh dish containing a grape juice-based medium overlaid with yeast. This procedure was replicated in five separate dishes for each strain.

After one day of egg laying, the number of eggs deposited was meticulously documented. Following this assessment, the female parents were relocated to a new dish. This egg quantification process was conducted over a total duration of eight days. For the virgin female, egg counts were performed every two days, extending over a span of ten days.

Quantification of offspring number per female fly

Newly hatched virgins were picked out and allowed to mature for two days in individual vials. They were then mated by placing one virgin female with three male flies for two days. After that, each female parent was transferred to a new vial and the number of offspring produced in 10 days was measured at 25°C and 29°C. All assays were performed with 20 females per genotype.

Measurement of starvation resistance in adult flies

We selected 3- to 5-day-old adult males and females and placed them in a starvation medium (1.5% agar), with 10 flies per vial and 10 vials for both males and females from each strain. We observed every 6 hours or 12 hours to count the number of deaths under starvation conditions until all flies starved to death. The survival curves were plotted by the ggsurvplot package in R.

Quantification and statistical analysis

Quantifications in all data graphs represent the mean of at least four biological replicates, and error bars represent the standard error of the mean (SEM). Two-tailed Mann-Whitney *U* test, Wilcoxon sign rank test, log-rank test, and two-tailed Student's *t* test were used to calculate significance. All statistical analysis was carried out using *Statskingdom*. In each statistical analysis, the number of biological replicates and significant *P* values were noted in corresponding Fig. legends.

Materials availability

All fly lines generated in this study are available from the Lead Contact.

858 **Table 1. uORFs in circadian rhythm genes.**

859

Description	Circadian rhythm genes	Core rhythm genes	*Clk*	*sgg*	*cwo*	*Pdp1*	*tim*	*cyc*	*vri*	*cry*	*Bdbt*	*per*
Total uORFs	1137	82	7	18	9	24	8	4	12	0	0	0
Conserved uORFs	29	7	1	1	1	4	0	0	0	0	0	0
Male head												
uORFs with mRNA RPKM > 0.1	888	67	6	15	8	24	6	3	5	0	0	0
uORFs with TE > 0.1	692	52	5	13	6	15	5	3	5	0	0	0
Conserved uORFs with mRNA RPKM > 0.1	28	7	1	1	1	4	0	0	0	0	0	0
Conserved uORFs with TE > 0.1	25	7	1	1	1	4	0	0	0	0	0	0
Female head												
uORFs with mRNA RPKM > 0.1	879	63	6	15	8	24	5	3	2	0	0	0
uORFs with TE > 0.1	714	49	6	13	5	16	5	3	1	0	0	0
Conserved uORFs with mRNA RPKM > 0.1	28	6	1	1	0	4	0	0	0	0	0	0
Conserved uORFs with TE > 0.1	25	6	1	1	0	4	0	0	0	0	0	0

860 The number of total uORFs or conserved uORFs in 169 circadian rhythm genes and ten core clock genes, as well as
861 each core clock gene, is shown. The number of transcribed and translated uORFs in heads of male and female flies
862 is shown. Conserved uORFs refer to the uATGs of uORFs that are present in all 23 *Drosophila* species. TE,
863 translational efficiency; RPKM, reads per kilobase of transcript per million mapped reads.

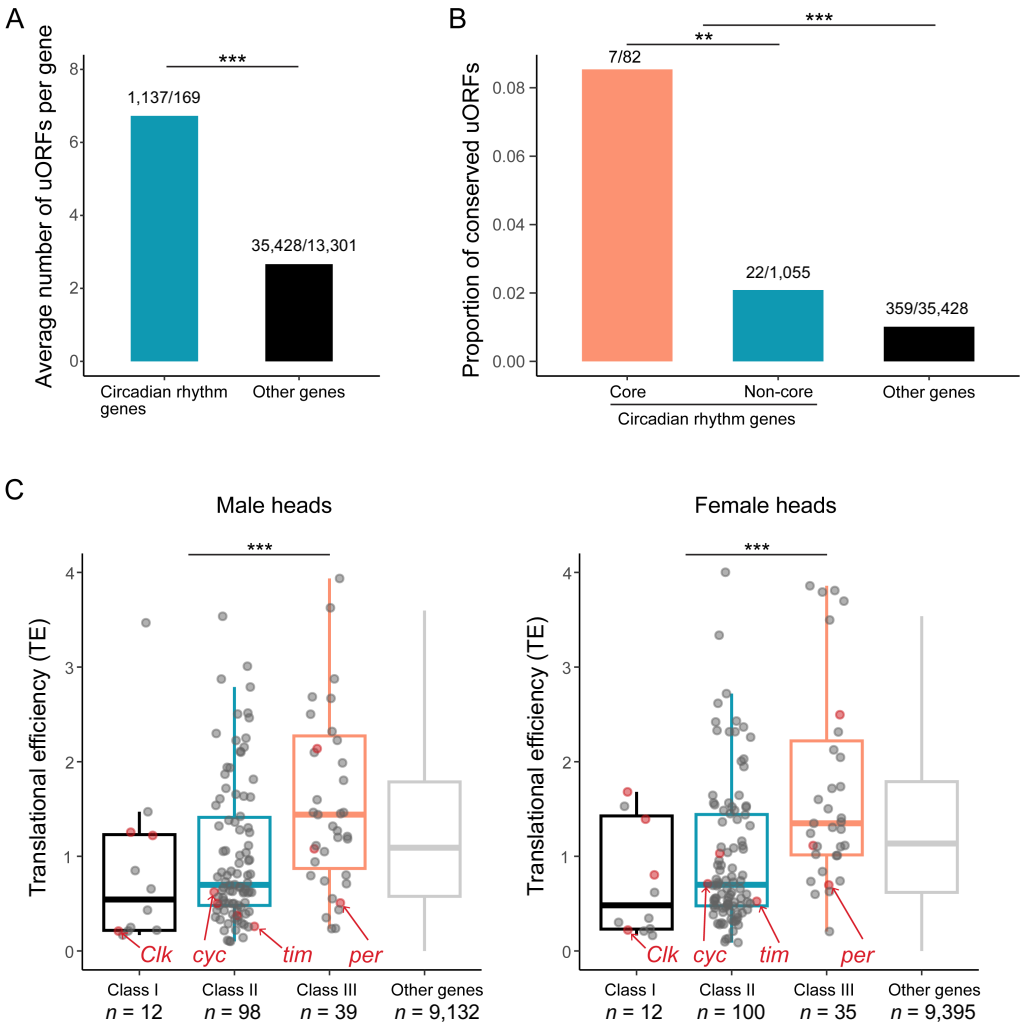

Fig. 1. Circadian rhythm genes are more likely to be regulated by uORFs.

(A) Average number of uORFs per gene for circadian rhythm-related genes and the other genes in *D. melanogaster*. The ratio of uORFs to genes is denoted on each bar (Fisher's exact test. ***, $P < 0.001$).

(B) Proportion of conserved uORFs in core clock genes, other circadian rhythm genes, and the other genes. Ratios reflect the number of conserved uORFs relative to the total count of uORFs for each category, depicted on each bar (Fisher's exact test. **, $P < 0.01$; ***, $P < 0.001$).

(C) The translational efficiency (TE) for different classes of circadian rhythm-related genes in male and female heads of *D. melanogaster*. Class I includes genes with conserved and translated uORFs. Class II consists of genes with non-conserved yet translated uORFs. Class III comprises genes without translated uORFs or lacking uORFs altogether. 'Other' encompasses all remaining genes expressed in heads that are not related to circadian rhythm. The gene counts of each class are denoted at the bottom of each bar. The ten core clock genes are highlighted with red dots, with *Clk*, *cyc*, *tim*, and *per* specifically marked by red arrows (Wilcoxon signed-rank test. ***, $P < 0.001$).

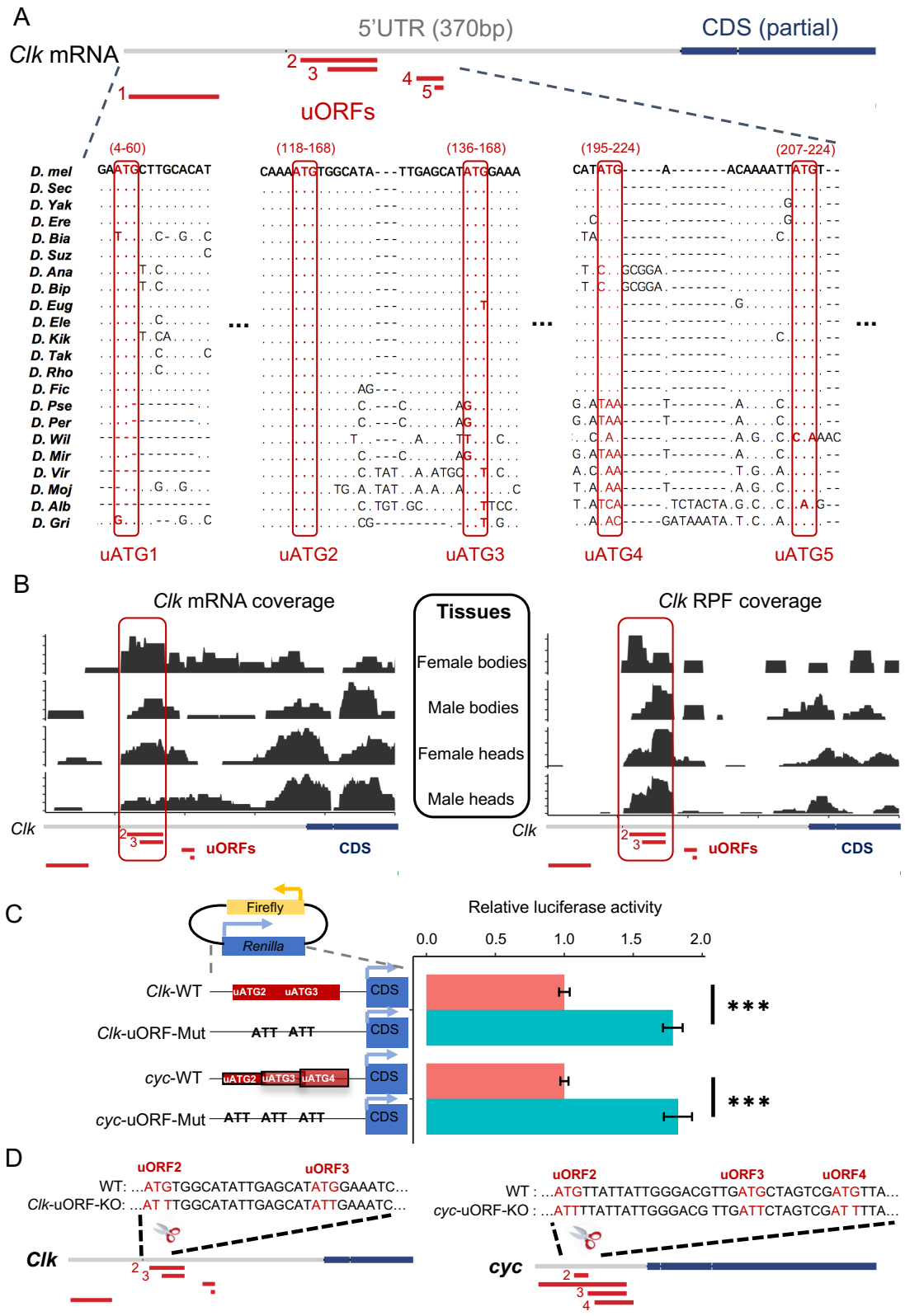

Fig. 2. Regulation of CLK and CYC Translation by uORFs in *Drosophila*.

(A) Multiple sequence alignment (MSA) of *Clk* uORFs among 23 *Drosophila* species. The start codons (uATGs) of uORFs are highlighted by red boxes. The position schemes of uORFs and partial CDSs are denoted above the MSA, with red and blue colors, respectively. The start and end positions of each uORF (separated by a "-") in the 5' UTR are given in the parenthesis

886 above each uATG.
887 (B) The mRNA reads coverage (left) and ribosome-protected footprints (RPF) coverage (right)
888 of uORFs of *Clk* mRNA from bodies and heads of both sexes. The position schemes of uORFs
889 and partial CDSs were denoted at the bottom.
890 (C) Dual-luciferase assays conducted on WT and uORF-mutated 5' UTRs of *Clk* and *cyc* genes
891 in *Drosophila* S2 cells, with reporter constructs depicted top left. For the uORF mutants, the
892 start codons of *Clk* uORF2 and uORF3, as well as *cyc* uORF2, uORF3, and uORF4, were
893 changed from ATGs to ATTs. Renilla luciferase activity was normalized against firefly
894 luciferase and the relative activity in WT was normalized to 1. Six replicates were conducted
895 for each experiment. Data represent mean ± SEM (Two-tailed Student's *t*-test; ***, $P < 0.001$).
896 (D) Diagrams depicting WT and two uORF knockout strains (*Clk*-uORF-KO and *cyc*-uORF-
897 KO), created using CRISPR-Cas9. For the uORF mutants, the start codons of *Clk* uORF2 and
898 uORF3, as well as *cyc* uORF2, uORF3, and uORF4, were simultaneously changed from ATGs
899 to ATTs. Below each sequence, uORFs (red boxes) and partial CDSs (blue boxes) are shown.
900

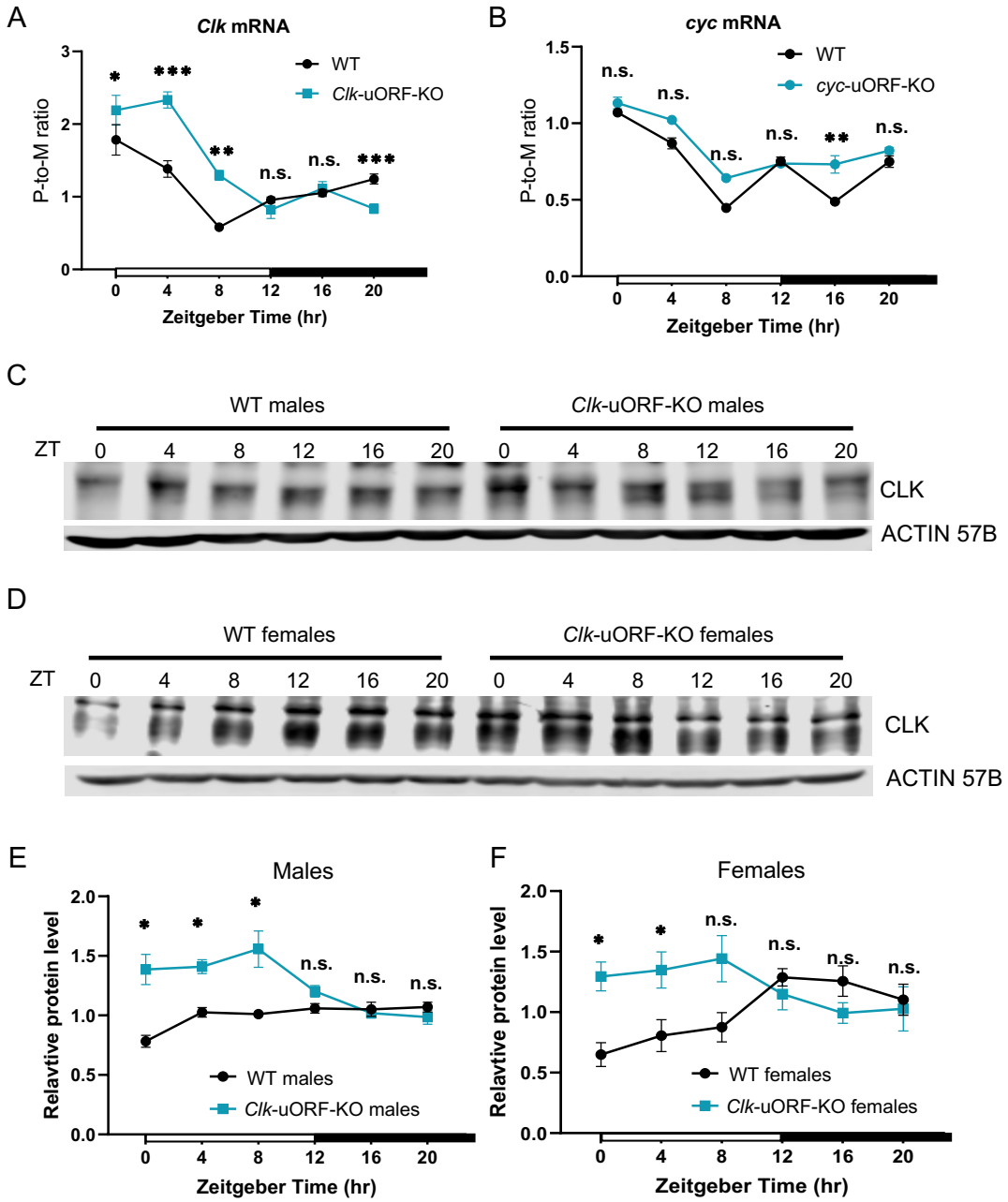

Fig. 3. *Clk* uORFs suppress CLK protein translation in fly heads *in vivo*.

(A) P-to-M ratios of *Clk* mRNA from whole heads of male *Clk*-uORF-KO compared to that in male WT flies, sampled at indicated Zeitgeber times at 4-hour intervals. Each time point includes six biological replicates. Data are expressed as mean ± SEM (Wilcoxon signed-rank test. *, $P < 0.05$; **, $P < 0.01$; ***, $P < 0.001$; n.s., $P > 0.05$).

(B) P-to-M ratios of *cyc* mRNA from whole heads of male *cyc*-uORF-KO compared to that in male WT flies, sampled at indicated Zeitgeber times at 4-hour intervals. Each time point includes six biological replicates. Data are expressed as mean ± SEM (Wilcoxon signed-rank test. **, $P < 0.01$; n.s., $P > 0.05$).

(C) Representative Western blots of CLK protein from whole-head protein extracts of male

flies, sampled at indicated Zeitgeber times at 4-hour intervals. ACTIN 57B served as the loading control.

(D) Representative Western blots of CLK protein from whole-head protein extracts of female flies, sampled at indicated Zeitgeber times at 4-hour intervals. ACTIN 57B served as the loading control.

(E) Quantification of CLK abundance relative to ACTIN 57B from (C), with the average intensity for WT normalized to 1 at each Zeitgeber Time (ZT) point. The analysis included four replicates. Data are presented as mean ± SEM (Two-tailed Mann-Whitney *U* test. *, $P < 0.05$; n.s., $P > 0.05$).

(F) Quantification of CLK abundance relative to ACTIN 57B from (D), with the average intensity for WT normalized to 1 at each Zeitgeber Time (ZT) point. The analysis included four replicates. Data are presented as mean ± SEM (Two-tailed Mann-Whitney *U* test. *, $P < 0.05$; **, $P < 0.01$; n.s., $P > 0.05$).

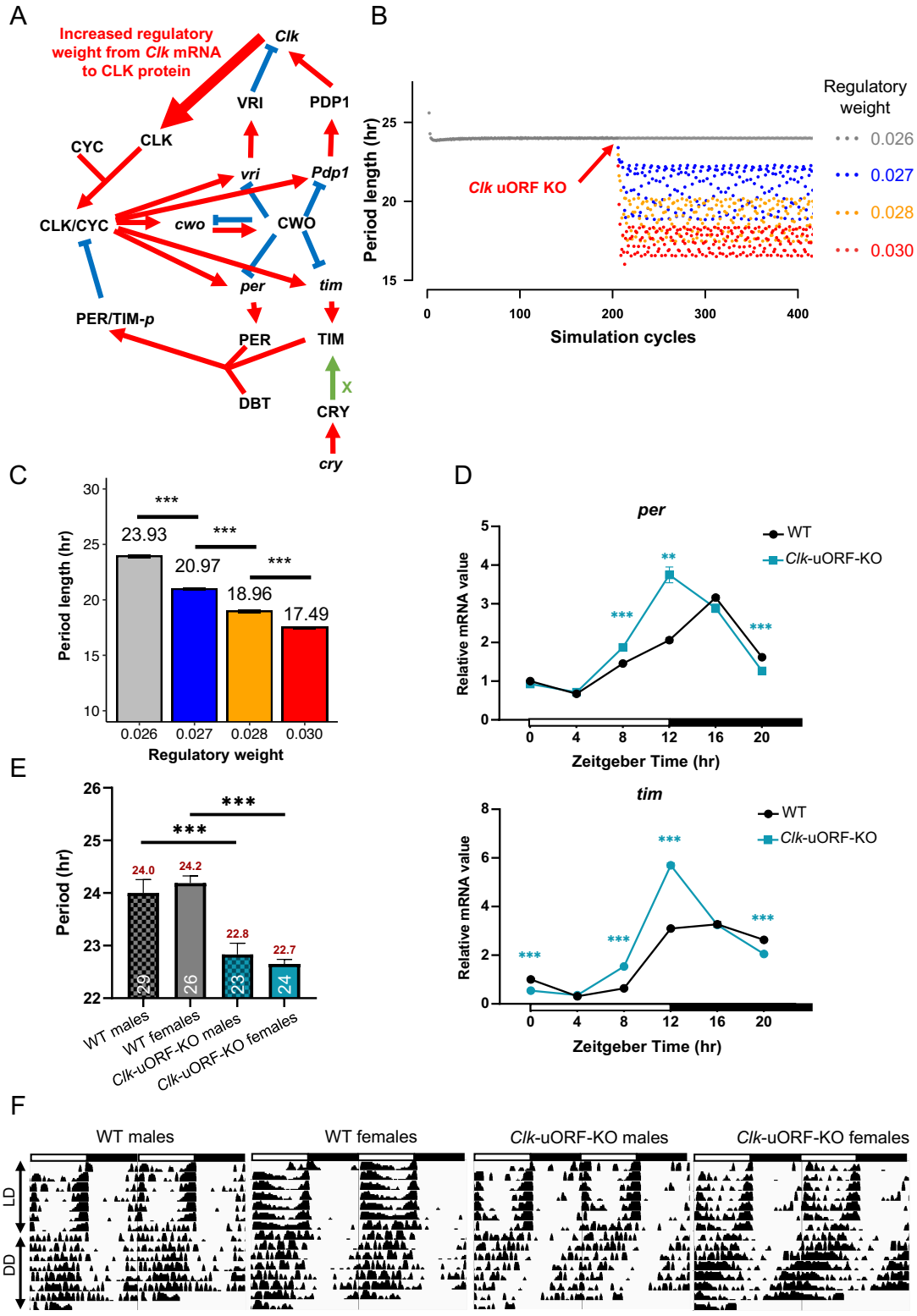

Fig. 4. Computational and experimental analysis of *Clk* uORFs on circadian rhythms. (A) Diagram of the *Drosophila* circadian clock molecular network, adapted from a previous study [47]. mRNA molecules are indicated in italicized lowercase, while protein molecules are in uppercase. Red arrows represent activation, while blue lines indicate suppression. The bold red arrow from *Clk* mRNA to CLK protein signifies the enhanced translation activity due to *Clk*

932 uORF knockout. The green arrow with an "X" indicates that CRY protein promotes the
933 degradation of TIM.
934 (B) The distribution of period length (hr) under different *Clk* mRNA to CLK protein regulatory
935 weights across approximately 400 simulation cycles. The original regulatory weight setting of
936 0.026 in the original model [47] acts as the baseline, emulating the presence of WT uORF. After
937 200 cycles the regulatory weight is increased from 0.0026 to several arbitrary higher levels
938 (0.027, 0.028, and 0.029) which is denoted by the red arrow, and continued for another 200
939 simulation cycles.
940 (C) The statistics of circadian period length (hr) for simulations in (B). Data are measured in
941 200 simulation cycles and are reported as the mean ± SEM (two-tailed Student's *t* test. ***, P
942 < 0.001).
943 (D) qRT-PCR measured mRNA levels of *per* and t*im* from total RNA extracts of female heads,
944 sampled at specified Zeitgeber time points. WT intensity at ZT0 is normalized to 1. Each time
945 point includes four biological replicates. Data are reported as the mean ± SEM (two-tailed
946 Student's *t* test. **, $P < 0.01$; ***, $P < 0.001$).
947 (E) Period of locomotor rhythms of *Clk*-uORF-KO flies and WT flies under constant darkness
948 conditions (DD). The period lengths (hr) and the number of flies tested (*n*) are displayed above
949 and below each bar, respectively.
950 (F) Representative double-plotted actograms of the locomotor activity of the indicated flies,
951 monitored under LD followed by DD. White and black bars represent light and dark phases,
952 respectively.
953
954
955

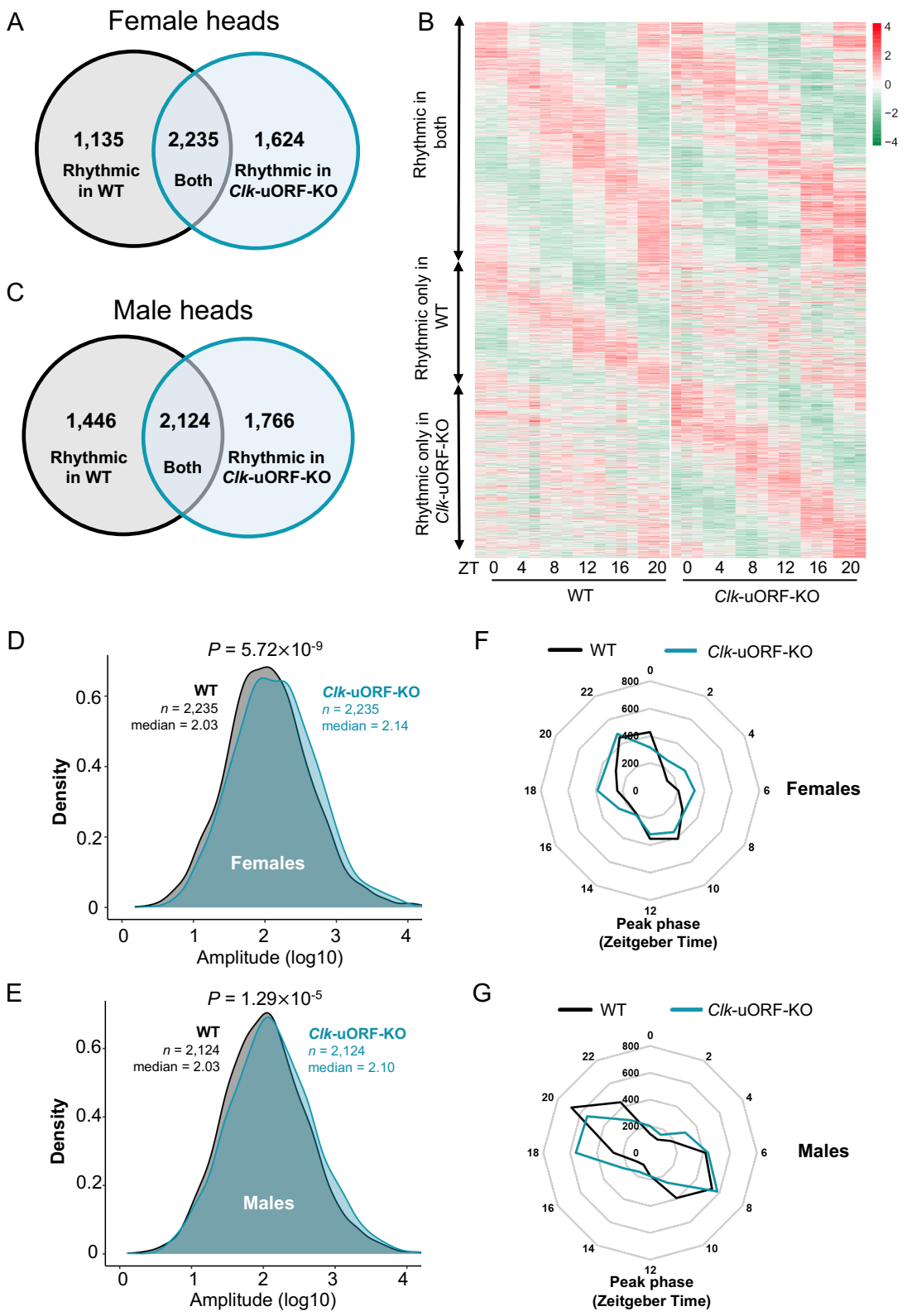

Figure 5. *Clk* uORFs modulate the temporal pattern of transcriptome expression landscape in fly heads.

(A) The number of rhythmically expressed genes identified from whole-head RNA-seq data of female WT and *Clk*-uORF-KO flies.

961 (B) Hierarchical clustering of genes expressed rhythmically in whole heads of female flies
962 across various Zeitgeber time points, with gene expression levels normalized to Z-scores. The
963 color scale reflects expression intensity, ranging from low (green) to high (red) Z-scores.
964 (C) The number of rhythmically expressed genes identified from whole-head RNA-seq data of
965 male WT and *Clk*-uORF-KO flies.
966 (D) The distribution of expression amplitudes for genes rhythmically expressed in the heads of
967 female WT and *Clk*-uORF-KO flies (n = 2,235; Wilcoxon rank sum test; $P = 5.72\times10^{-9}$).
968 (E) The distribution of expression amplitudes for genes rhythmically expressed in the heads of
969 male WT and *Clk*-uORF-KO flies (n = 2,124; Wilcoxon rank sum test; $P = 1.29\times10^{-5}$).
970 (F-G) Phase distribution of rhythmically expressed genes in whole heads of female WT and
971 *Clk*-uORF-KO flies (F) and male WT and *Clk*-uORF-KO flies (G). The y-axis of the radar chart
972 indicates the number of rhythmic genes.

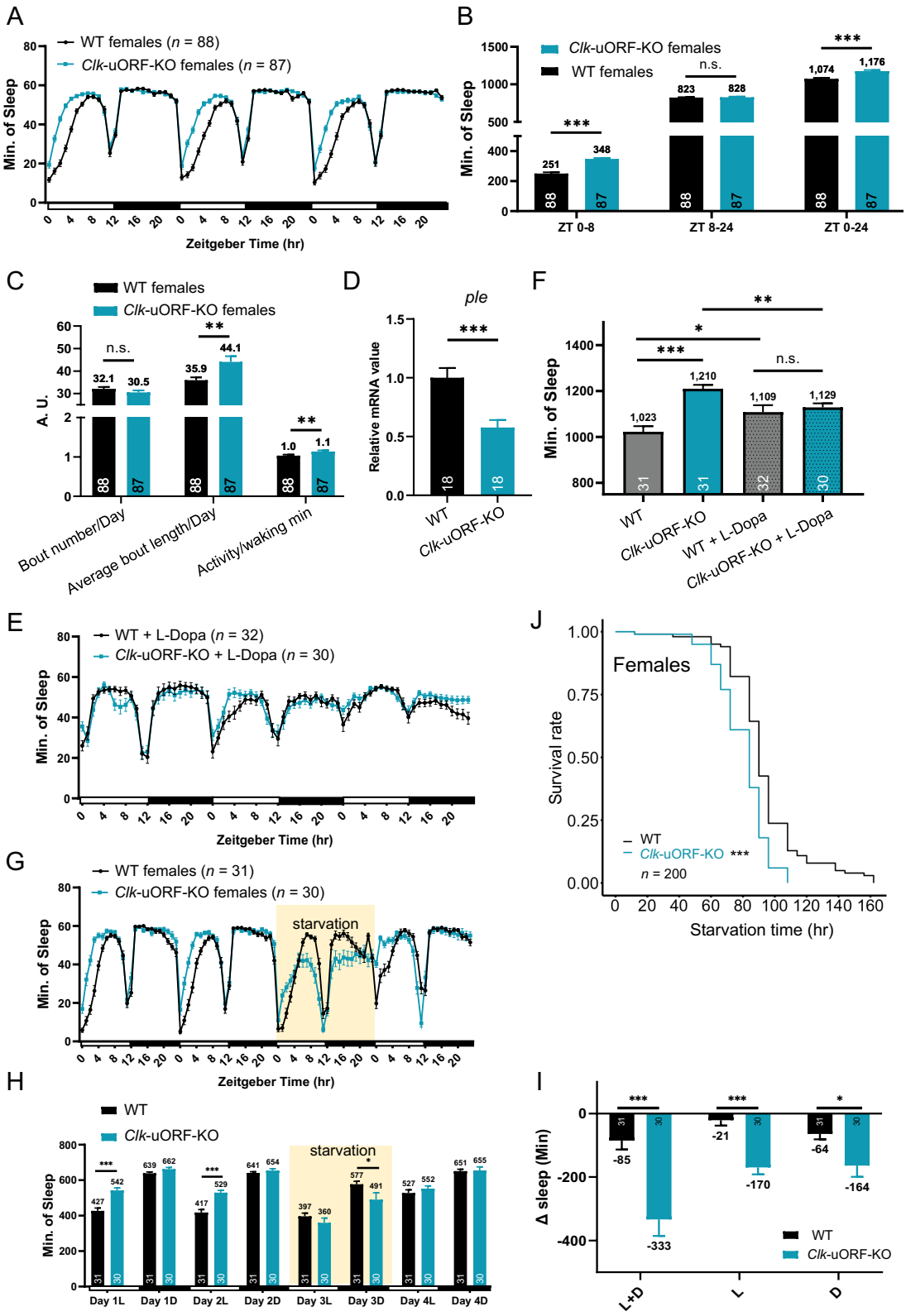

Fig. 6. *Clk* uORFs regulate sleep/wakefulness.

(A) Sleep profile of female *Clk*-uORF-KO and WT flies under LD conditions.

(B) Sleep duration during ZT0-8, ZT8-24, and ZT0-24 of female *Clk*-uORF-KO and WT flies under LD condition.

(C) Daily sleep bout number, average bout length, and average waking activity of female *Clk*-

uORF-KO and WT flies under LD condition.

(D) The relative mRNA abundance of *ple* determined by RT-qPCR using whole-head total RNA extracts collected from female flies under LD conditions. The average value of WT is set to 1.

(E) Sleep profile of female *Clk*-uORF-KO and WT flies treated with L-Dopa under LD condition.

(F) Daily sleep duration of female *Clk*-uORF-KO *vs.* WT flies treated with L-Dopa.

(G) Sleep profile of female uORF-KO and WT flies under food ad libitum and starvation (the 3rd day) condition. The yellow shade indicates period of starvation.

(H) Daily sleep duration of female *Clk*-uORF-KO and WT flies under baseline and starvation conditions.

(I) Histogram shows starvation-induced sleep change (Δ sleep) compared with normal conditions during daytime (L), nighttime (D), and the entire day (LD).

(J) Survival curves of female flies under starvation conditions (n = 200; log-rank test; ***, P < 0.001).

The numbers of flies tested are shown in the brackets of legend or the bottom of histograms. Data are presented as the mean ± SEM. Asterisks indicate statistical significance (two-tailed Student's t test. *, $P < 0.05$; **, $P < 0.01$; ***, $P < 0.001$; n.s., $P > 0.05$). ZT, Zeitgeber Time.

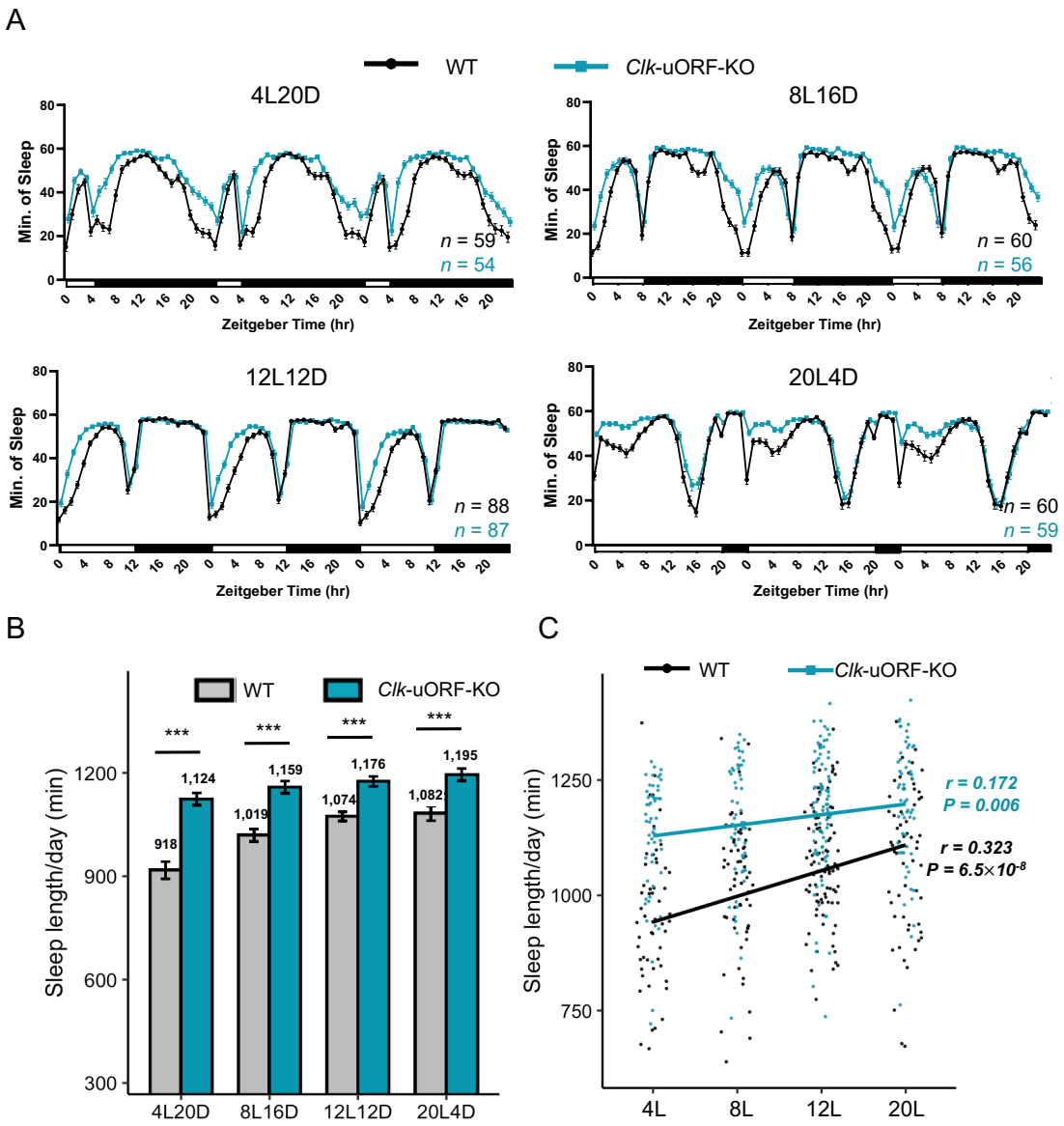

Fig. 7. *Clk* uORFs promote wakefulness in adaptation to seasonal photoperiod changes. (A) Sleep profile of female *Clk*-uORF-KO and WT flies under 4 h L : 20 h D (4L20D) (A), 8 h L : 16 h D (8L16D) (B), 12 h L : 12 h D (12L12D) (C), and 20 h L : 4 h D (20L4D) (D) condition. The numbers of tested flies (*n*) are shown in the bottom-right.

(B) Daily sleep duration (min) of female *Clk*-uORF-KO and WT flies under different photoperiods. Data are presented as the mean ± SEM. Asterisks and dollar signs indicate statistical significance (two-tailed Student's *t* test. ***, $P < 0.001$).

(C) The correlation between daily sleep duration (min) and photoperiod length in female *Clk*-uORF-KO and WT flies (Pearson's correlation).

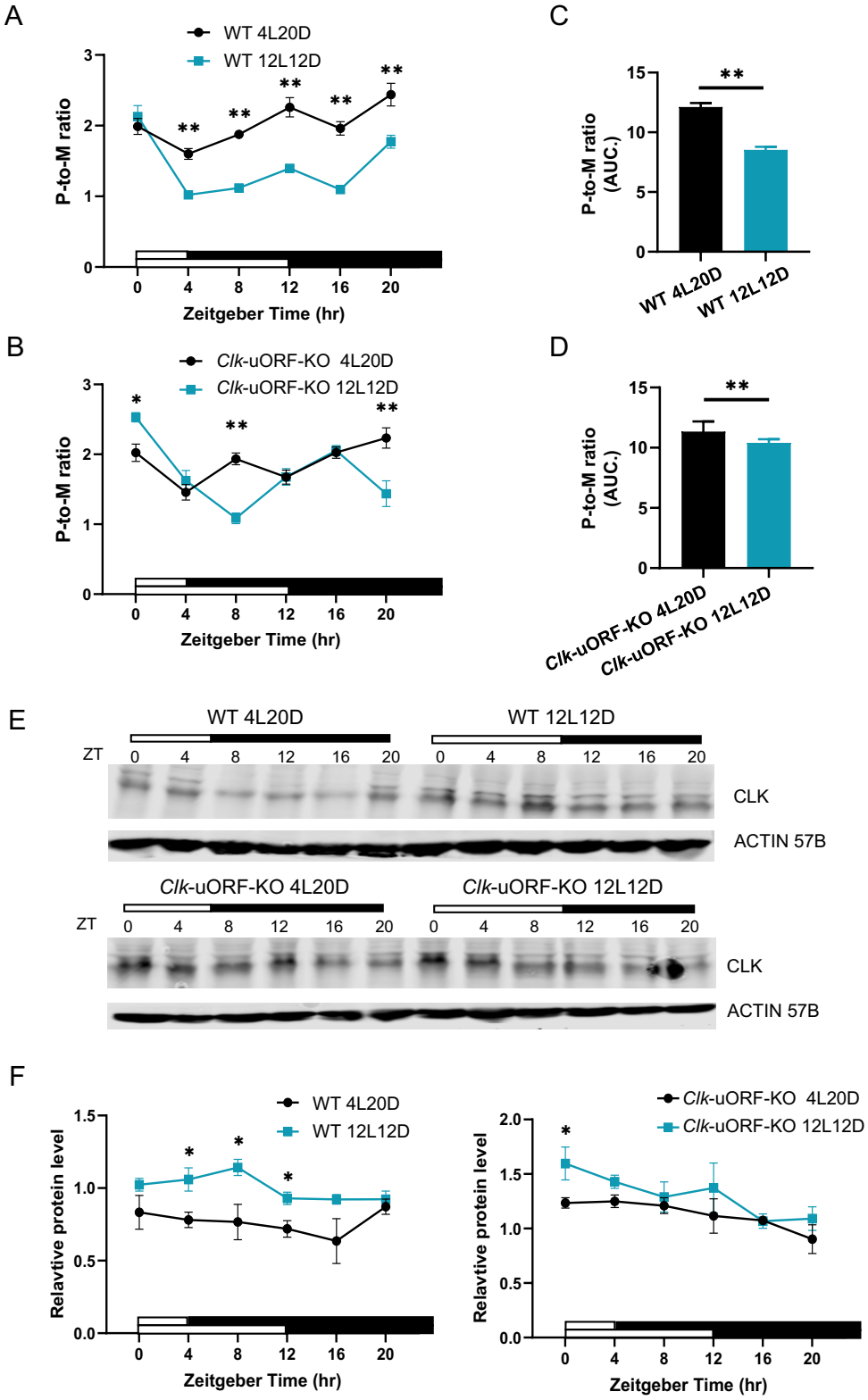

Fig. 8. *Clk* uORFs suppress CLK protein translation in a photoperiod-dependent manner. (A-B) P-to-M ratios of *Clk* mRNA from whole-head extracts collected from female WT (A) and *Clk*-uORF-KO (B) flies at indicated time points under 4L20D and 12L12D conditions. Each time point includes six biological replicates and data are presented as the mean ± SEM. (C-D) AUC analysis of daily P-to-M ratio in (A) and (B) of female WT (C) and *Clk*-uORF-KO

1013 (D) flies under indicated photoperiod.

1014 (E) Representative Western blots for CLK protein from whole-head total protein extracts
1015 collected from female WT (upper) and *Clk*-uORF-KO (lower) flies at indicated time points
1016 under 4L20D (left) and 12L12D (right). ACTIN 57B is used as a loading control.

1017 (F) The relative CLK abundance normalized to ACTIN 57B in (E). The average value of WT
1018 under 12L12D is set to 1. Each time point includes four biological replicates and data are
1019 presented as the mean ± SEM.

1020 Asterisks indicate statistical significance (two-tailed Mann-Whitney *U* test for unpaired
1021 comparisons. **, $P < 0.01$; ***, $P < 0.001$). ZT, Zeitgeber Time.

1022